

Time delayed control of structural systems

Firdaus E. Udwadia^{1,*}, Hubertus F. von Bremen², Ravi Kumar³
and Mohammad Hosseini²

¹*Department of Civil Engineering, Aerospace and Mechanical Engineering, Mathematics, and Information and Operations Management, University of Southern California, Los Angeles, CA 90089-1453, U.S.A.*

²*Department of Aerospace and Mechanical Engineering, University of Southern California, Los Angeles, CA 90089-1453, U.S.A.*

³*Structural Analysis and Research Corporation, 5000 McKnight Road, Pittsburgh, PA 15237, U.S.A.*

SUMMARY

Time delays are ubiquitous in control systems. They usually enter because of the sensors and actuators used in them. Traditionally, time delays have been thought to have a deleterious effect on both the stability and the performance of controlled systems, and much research has been done in attempting to eliminate them, compensate for them, or nullify their presence. In this paper we take a different view. We investigate whether purposefully injected time delays can be used to *improve* both the system's stability and performance. Our analytical, numerical, and experimental investigation shows that this can indeed be done. Analytical results of the effects of time delays on collocated and non-collocated control of classically damped and non-classically damped systems are given. Experimental and numerical results confirm the theoretical expectations. Issues of system uncertainties and robustness of time delayed control are addressed. The results are of practical value in improving the performance and stability of controllers because these characteristics (performance and stability) improve *dramatically* with the intentional injection of small time delays in the control system. The introduction of such time delays constitutes a 'minimal change' to a controller already installed in a structural system for active control. Hence, from a practical standpoint, time delays can be implemented in a nearly costless and highly reliable manner to improve control performance and stability, an aspect that cannot be ignored when dealing with the economics and safety of large structural systems subjected to strong earthquake ground shaking. Copyright © 2003 John Wiley & Sons, Ltd.

KEY WORDS: time delayed control; structural systems; collocated and non-collocated control; classically damped and non-classically damped systems; stability; theory, experiment, and simulations; uncertain systems and time delays

1. INTRODUCTION

The active control of large-scale structural systems usually requires the generation of large control forces which often need to be provided at high frequencies. Actuator and sensor

* Correspondence to: Firdaus E. Udwadia, Department of Aerospace and Mechanical Engineering, University of Southern California, Los Angeles, CA 90089-1453, U.S.A.

† E-mail: fudwadia@usc.edu

Received 16 March 2001

Revised 8 May 2002

Accepted 8 June 2002

dynamics do not permit the instantaneous generation of such forces and hence the effective control gets delayed in time. Thus the presence of time delays in the control are inevitable when controlling building structures subjected to dynamic loads, such as those caused by strong earthquake ground shaking. In order to accommodate for the time delays, the mathematical formulations of the problem of controlling building structures are usually more complicated than the formulations without time delays. The fact that the models are more complicated when time delays are included and that in some cases the presence of time delays destabilize the control has fueled the predominant view that time delays are an undesirable element in the active control of structures. With this view in mind, methods to cancel out, reduce, or change the effect of time delays have been developed. This paper proposes a different viewpoint: its central theme is that instead of considering time delays as always being injurious, one could aim to exploit their presence, especially since they are ubiquitous. We show that the proper intentional introduction of time delays: (1) can stabilize even a non-collocated control system (which may be unstable in the absence of time delays), and (2) may improve control performance.

Extensive work has been done on the control of structural systems where no consideration to time delays is given. The fact that the results do not include time delays does not undermine their importance when controlling large building structures, since several of the concepts can be used as a starting point when dealing with time-delayed problems. Feedback control of structural systems yields different stability characteristics depending on whether collocated or non-collocated control is used. Direct velocity feedback (no time delay) control of a discrete dynamical system with collocation of actuators and sensors is known to be stable for all values of the control gain [1, 2]. Balas [3] has investigated the potential of direct output feedback control for systems where sensors and actuators need not be collocated. When actuators' dynamics are considered, Goh and Caughey [4] and Fanson and Caughey [5] have shown that position feedback is preferable to velocity feedback under collocated control. Cannon and Rosenthal [6] deal with experimental studies of collocated and non-collocated control of flexible structures. Based on these studies, it has been concluded that it is very difficult to achieve robust non-collocated control of flexible structures.

In practical feedback control systems, small time delays in the control action are inevitable because of the involved dynamics of the actuators and sensors. As stated before, these time delays become particularly significant when the control effort demands large control forces, and/or high frequencies. It is therefore crucial to understand the effect of time delays on the control of structural systems. Several papers in the literature treat the presence of time delays as a negative factor. Yang *et al.* [7] show that time delays worsen performance for their proposed controllers. Agrawal and Yang [8] show through simulations that the degradation of the control performance of an actively controlled structural system due to a fixed time delay is not significant until the delay reaches a critical value. Agrawal *et al.* [9] and Agrawal and Yang [10] indicated methods of compensation for time delay in the active control of structural systems. On the other hand, some previous studies suggest that time delays can be used to good advantage. Kwon *et al.* [11] show that the intentional use of time delays may improve the performance of the control system. Udwadia and Kumar [12] show that dislocated velocity control, which leads to instability in the absence of time delays, can be used to even stabilize an MDOF system (for small gains) by an appropriate choice of time delays. In the present paper (Section 3) we show that the intentional injection of time delays can increase the maximum gain for stability of a non-classically damped system (when compared with

the system with no time delays). Experimental results on a two-degree-of-freedom torsional system (Section 4) confirm our analytical findings and show that it is possible to choose time delays which improve the controller's performance when compared to the controlled system with no time delays.

This paper is organized as follows. Section 2 of the paper deals with the time-delayed control of classically damped systems. Results for collocated as well as for non-collocated control of undamped and underdamped systems are given. The theoretical expectations are confirmed numerically when applied to a building structure model which is subjected to an earthquake. Numerical results on the sensitivity of the control methodology to perturbations (a) of the parameters of a building structure, and (b) of the time delays used are also presented. Section 3 deals with more general, non-classically damped, linear systems. Section 4 presents experimental data on a two degree-of-freedom non-classically damped torsional system. Numerical results which corroborate the theoretical findings obtained in the previous sections are also presented for comparison. Here we also show that it is possible for a non-system pole (a pole whose root locus does not start at an open loop pole of the structural system) to dictate the maximum gain for stability of the time-delayed, controlled system. Section 5 presents robustness issues. It deals with the control of uncertain systems with uncertain time varying delays in the control input. Our conclusions are presented in Section 6.

2. CLASSICALLY DAMPED STRUCTURAL SYSTEMS

This section deals with the time-delayed control of classically damped structures. Collocated as well as non-collocated control of undamped and underdamped structures are considered. Most of the results apply to controllers of the PID type (proportional, integral, derivative). Numerical computations are used to confirm some of the theoretical expectations for a building structure subjected to an earthquake. Most of the results apply only to the case when system poles are considered (that is, for poles whose root locus originates at the open loop poles of the structural system). The sensitivity of the stability of the building structure when the parameters of the structure and the time delay are varied is explored numerically. It is shown numerically that even under considerable perturbations (7–50%) of the parameter values the system remains stable. Details of some of the analytical results presented in this section can be found in Udawadia and Kumar [12] and part of the numerical results can be found in Udawadia and Kumar [13].

2.1. System model and general formulation

Consider a linear classically damped structural system whose response $x(t)$ is described by the matrix differential equation

$$Mx''(t) + Cx'(t) + Kx(t) = g(t); \quad x(0) = 0, \quad x'(0) = 0 \quad (1)$$

where M is the $n \times n$ positive definite symmetric mass matrix, C is the $n \times n$ symmetric damping matrix, and K is the $n \times n$ positive definitive symmetric stiffness matrix. The forcing function is given by the n -vector $g(t)$.

Since the system is classically damped, it can be transformed to the diagonal system

$$z''(t) + \Xi z'(t) + \Lambda z(t) = T^T M^{-1/2} g(t); \quad z(0) = 0, \quad z'(0) = 0 \tag{2}$$

where $\Xi = \text{diag}(2\xi_1, 2\xi_2, \dots, 2\xi_n)$, $\Lambda = \text{diag}(\lambda_1^2, \lambda_2^2, \dots, \lambda_n^2)$, and the matrix $T = [t_{ij}]$ is the orthogonal matrix of eigenvectors of $M^{-1/2}KM^{-1/2}$. Taking the Laplace transform of Equation (2) and solving, we get

$$\tilde{x}(s) = M^{-1/2} T \Theta T^T M^{-1/2} \tilde{g}(s) \tag{3}$$

where the wiggles indicate the transformed functions, and Θ is given by

$$\Theta = \text{diag}((s^2 + 2\xi_1 s + \lambda_1^2)^{-1}, (s^2 + 2\xi_2 s + \lambda_2^2)^{-1}, \dots, (s^2 + 2\xi_n s + \lambda_n^2)^{-1})$$

The open loop poles are given by the zeros of the equations

$$s^2 + 2\xi_q s + \lambda_q^2 = (s - \gamma_{+q})(s - \gamma_{-q}) = 0, \quad q = 1, 2, \dots, n \tag{4}$$

The poles have been denoted by $\gamma_{\pm q}$, the sign indicating the sign in front of the radical of the quadratic equations given in Equation (4). In this paper we assume the system to be generic and all poles to have multiplicity one (no repeated poles).

The feedback control uses a linear combination of p responses $x_{s_k}(t)$, $k = 1, 2, \dots, p$, which are fed to a controller. In general, the responses are time-delayed by T_{s_k} . The actuator will apply a force to the system, affecting the j th equation of Equation (1). When $j \in \{s_k : k = 1, 2, \dots, p\}$ the sensors and the actuator are collocated, and if $j \notin \{s_k : k = 1, 2, \dots, p\}$ the sensors and the actuator are non-collocated (dislocated). The control methodology applied to a shear frame building structure is shown in Figure 1.

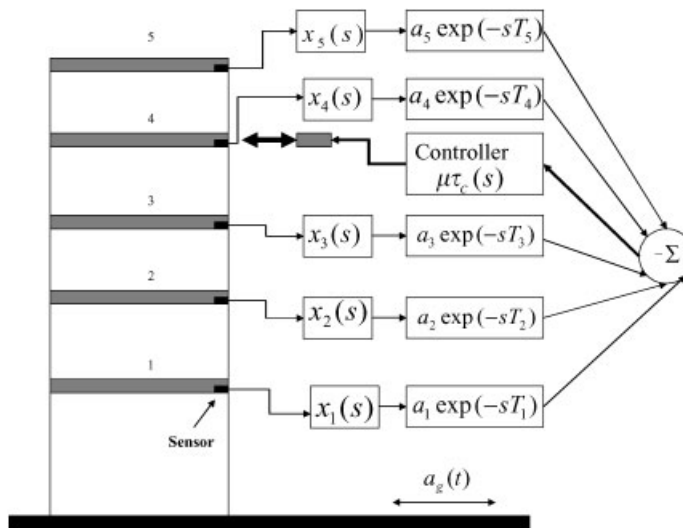


Figure 1. Shear frame building structure and control methodology.

Denoting the non-negative control gain by μ and the controller transfer function by $\mu\tau_c(s)$, the closed loop system poles are given by

$$\tilde{A}(s)\tilde{x}(s) = [Ms^2 + Cs + K]\tilde{x}(s) = \tilde{g}(s) - \mu\tau_c(s) \sum_{k=1}^p a_{s_k} \tilde{x}_{s_k}(s) \exp[-sT_{s_k}]e_j \tag{5}$$

where e_j is the unit vector with unity in the j th element and zeros elsewhere. The numbers a_{s_k} are the coefficients of the linear combination of the responses fed to the controller. Moving the last term on the right of Equation (5) to the left gives

$$\tilde{A}_1(s)\tilde{x}(s) = \tilde{g}(s) \tag{6}$$

where $\tilde{A}_1(s)$ is obtained by adding $\mu\tau_c(s)a_{s_k} \exp[-sT_{s_k}]$ to the (j, s_k) th element of $\tilde{A}(s)$, for $k=1, 2, \dots, p$.

The closed loop poles are then given by the relation

$$\det[\tilde{A}_1(s)] = \det[\tilde{A}(s)] \left\{ 1 + \mu\tau_c(s) \sum_{k=1}^p a_{s_k} \exp[-sT_{s_k}] \tilde{x}_{s_k,j}^{(\delta)}(s) \right\} = 0 \tag{7}$$

where $\tilde{x}_{s_k,j}^{(\delta)}(s)$ is the Laplace transform of the open loop response to an impulsive force applied at node j at time $t=0$. The open loop response to the impulsive force is given by

$$\tilde{x}_{s_k,j}^{(\delta)}(s) = \sum_{i=1}^n \frac{t_{s_k,i}^{(M)} t_{j,i}^{(M)}}{s^2 + 2\zeta_i s + \lambda_i^2}$$

where

$$t_{s_k,r}^{(M)} = \sum_{u=1}^n m_{s_k,u}^{-1/2} t_{u,r}$$

with $m_{i,j}^{-1/2}$ being the (i, j) th element of $M^{-1/2}$ and $T^{(M)} = M^{-1/2}T = [t_{i,j}^{(M)}]$.

The following set of conditions will be referred to as condition set C1. Given that the open loop poles of the system are $\gamma_{\pm q}$, we have

- (1) $\tau_c(\gamma_{\pm q}) \neq 0$, for $q = 1, 2, \dots, n$
- (2) $\sum_{k=1}^p a_{s_k} \exp[-\gamma_{\pm q} T_{s_k}] t_{s_k,q}^{(M)} \neq 0$, for $q = 1, 2, \dots, n$
- (3) $t_{j,q}^{(M)} \neq 0$, for $q = 1, 2, \dots, n$

The first condition means that the open loop poles of the system are not also zeros of the controller transfer function. The second condition is a generalized observability condition which requires that all mode shapes are observable from the summed, time-delayed sensor measurements. The third condition is a controllability condition which requires that the controller cannot be located at any node of any mode of the system. Observe that if any of the three conditions is not satisfied for one open loop pole γ_q , then by Equation (7) the open loop pole γ_q is also a closed loop pole. However, if C1 is satisfied, we have the following result.

Result 2.1

When the open loop system has distinct poles and condition set C1 is satisfied, the open loop and the closed loop systems have no poles in common.

If condition set C1 is satisfied, then by Result 2.1 and Equation (7), the closed loop poles of the system are given by the values of s that satisfy the equation

$$1 + \mu\tau_c(s) \sum_{k=1}^p \sum_{i=1}^n a_{s_k} \exp[-sT_{s_k}] \left[\frac{t_{s_k,i}^{(M)} t_{j,i}^{(M)}}{s^2 + 2\xi_i s + \lambda_i^2} \right] = 0 \quad (8)$$

In general, Equation (8) may have an infinite number of zeros due to the time delay term. As the parameter μ is varied, we obtain the root locus of the closed loop poles. The poles that are on a root locus that starts at an open loop pole of the structural system will be called system poles. The poles that do not originate at an open loop pole of the system will be called non-system poles. To simplify matters, some of the following results deal with the system poles only. The simplification of dealing with the system poles only, allows us to obtain bounds on the gain and the time delay to guarantee stability. These results should be viewed with caution since in general there are an infinite number of poles, and as shown in Section 4, a non-system pole may determine what is the maximum gain for stability for some systems. It will be made clear when our results apply to all the poles considered, and when only to the system poles.

The following result and all of its consequences apply to the case when only system poles are considered. Multiplying Equation (8) by $s^2 + 2\xi_r s + \lambda_r^2$, then differentiating with respect to μ and letting $s \rightarrow \gamma_{\pm r} = -\xi_r \pm i(\lambda_r^2 - \xi_r^2)^{1/2}$ and $\mu \rightarrow 0$, we obtain

$$\left. \frac{ds}{d\mu} \right|_{\substack{\mu \rightarrow 0 \\ s \rightarrow \gamma_{\pm r}}} = - \frac{\tau_c(\gamma_{\pm r})}{\pm 2i(\lambda_r^2 - \xi_r^2)^{1/2}} \left[\sum_{k=1}^p a_{s_k} \exp[-\gamma_{\pm r} T_{s_k}] t_{s_k,r}^{(M)} \right] t_{j,r}^{(M)} \quad (9)$$

Result 2.2

A sufficient condition for the closed loop system to remain stable for infinitesimal gains is that

$$Re \left\{ \left. \frac{ds}{d\mu} \right|_{\substack{\mu \rightarrow 0 \\ s \rightarrow \gamma_{\pm r}}} \right\} < 0, \quad r = 1, 2, \dots, n \quad (10)$$

Again, Result 2.2 applies only when system poles are considered, and in general the result may not be true when non-system poles are also considered.

We now particularize the controller to be of the proportional, integral and derivative (PID) form. The transfer function of the controller is then given by

$$\tau_c(s) = K_0 + K_1 s + \frac{K_2}{s} \quad \text{with } K_0, K_1, K_2 \geq 0$$

The term K_0 corresponds to proportional control, the term $K_1 s$ corresponds to derivative control and the term K_2/s corresponds to integral control. Next we specialize results for the undamped case.

2.2. Undamped systems

The following set of results apply to undamped systems. When the damping matrix $C=0$, the open loop poles lie on the imaginary axis, and by Equation (10), the next result follows.

Result 2.3

For undamped systems ($C=0$), condition (10) is a necessary and sufficient condition for stability for small gains.

For an undamped system, the open loop poles are of the form $\gamma_{\pm r} = \pm i\lambda_r$. Using Equations (9) and (10) we can derive the following requirement for stability for small gains (this result applies to system poles only).

$$\operatorname{Re} \left\{ \left(\frac{K_0}{\pm i\lambda_r} + K_1 - \frac{K_2}{\lambda_r^2} \right) \left(\sum_{k=1}^p a_{s_k} \exp[\mp i\lambda_r T_{s_k}] t_{s_k, r}^{(M)} t_{j, r}^{(M)} \right) \right\} > 0 \quad (11)$$

for $r = 1, 2, \dots, n$.

Using relation (11), we can derive the following result.

Result 2.4

When using one sensor collocated with the actuator for an undamped system, the PID feedback control is stable (for small gains) if and only if

$$a_j \left\{ -\frac{K_0}{\lambda_r} \sin(\lambda_r T_j) + \left(K_1 - \frac{K_2}{\lambda_r^2} \right) \cos(\lambda_r T_j) \right\} > 0 \quad (12)$$

for $r = 1, 2, \dots, n$.

Result 2.5

For undamped systems with one sensor collocated with the actuator, we have the following conditions for stability for small gains.

- (a) Velocity feedback ($K_0 = K_2 = 0$) is stable as long as the time delay is such that $T_j < \pi/2\lambda_{\max}$, where λ_{\max} is the highest undamped natural frequency of the system.
- (b) Integral control ($K_0 = K_1 = 0$) is stable as long as the delay is such that $T_j < \pi/2\lambda_{\max}$.
- (c) Proportional control ($K_1 = K_2 = 0$) is stable as long as the delay is such that $0 < T_j < \pi/\lambda_{\max}$.
- (d) When $K_0 = 0$ and the time delay is such that $T_j < \pi/2\lambda_{\max}$, the undamped system will be stabilized when $K_1 > K_2/\lambda_{\min}^2$ and $a_j > 0$, or $K_1 < K_2/\lambda_{\max}^2$ and $a_j < 0$.

Result 2.6

When the system is undamped, and

- (1) condition set C1 is satisfied,
- (2) one sensor is used and is collocated with the actuator, and,
- (3) no time delay is used,

then the PID control, if stable for $\mu \rightarrow 0^+$ is stable for all $\mu > 0$, provided

$$\det \left[\tilde{A} \left(-\frac{K_2}{K_1} \right) \right] + \mu a_j K_0 \det \left[\tilde{A}_2 \left(-\frac{K_2}{K_1} \right) \right] \neq 0 \quad (13)$$

for any positive μ , where \tilde{A}_2 is obtained by deleting the j th row and the j th column of the matrix \tilde{A} .

When velocity (or integral) feedback control is used, condition (13) is always satisfied, hence we get the well-known result that stability is guaranteed for $\mu > 0$. The upper bound for the stability of the system described in Result 2.6 can be obtained to be

$$\mu < \frac{-\det[\tilde{A}(-K_2/K_1)]}{a_j K_0 \det[\tilde{A}_2(-K_2/K_1)]}$$

provided the right-hand side in the inequality is positive. If not, the system is stable for all $\mu > 0$, provided it is stable for small gains. Result 2.6 and the above bound on the gain for stability apply to the case when all the poles are considered. The next result however only applies when system poles are considered.

Result 2.7

When the system is undamped, and

- (1) condition set C1 is satisfied,
- (2) one sensor is used and it is collocated with the actuator, and
- (3) time delay $T_j < \pi 2\lambda_{\max}$,

then velocity feedback control will be stable as long as

$$\mu < \frac{1}{a_j K_1 \eta_0 \sum_{i=1}^n [t_{j,i}^{(M)}]^2 / (\eta_0^2 - \lambda_i^2)} \quad \text{where } \eta_0 = \pi/2T_j$$

The previous results have focused on collocated control. In the following results we will consider the control of non-collocated (dislocated) systems. Results dealing with no time delay are presented first, and are followed by results for time-delayed systems.

Result 2.8

When using a PID controller, where

- (1) the sensors and the actuator are not collocated,
- (2) the time delays, T_{s_k} , $k = 1, 2, \dots, p$, are all zero,
- (3) the matrix M is diagonal, and
- (4) $K_1 > K_2/\lambda_{\min}^2$ or $K_1 < K_2/\lambda_{\max}^2$,

it is impossible to stabilize the undamped system for small gains.

The next result gives necessary conditions for the stability of a system using a PID controller.

Result 2.9

When using a PID controller, where

- (1) the sensors and the actuator are not collocated,
- (2) the time delays, T_{s_k} , $k = 1, 2, \dots, p$, are all zero, and
- (3) the matrix M is non-diagonal,

a necessary condition for the undamped system to be stabilized for small gains is

- (a) $\sum_{k=1}^p a_{s_k} m_{s_k, j}^{-1} > 0$ when $K_1 > K_2 / \lambda_{\min}^2$, and
- (b) $\sum_{k=1}^p a_{s_k} m_{s_k, j}^{-1} < 0$ when $K_1 < K_2 / \lambda_{\max}^2$.

Often building structures are modelled by tridiagonal stiffness matrices. The following result applies to such structures.

Result 2.10

If M and K are positive definite, M is diagonal and K is tridiagonal, having negative sub-diagonal elements, it is possible to find a location j (for the actuator) and a location s_l (for the sensor), $j \neq s_l$, so that the sequence $\{t_{s_l, i}^{(M)}, t_{j, i}^{(M)}\}_{i=1}^n$ will only have one sign change.

Result 2.11

When using an ID controller, for a system as defined in Result 2.10, where

- (1) condition set C1 is satisfied,
- (2) one sensor is used and it is not collocated with the actuator,
- (3) the sign change in the sequence $\{t_{s_l, i}^{(M)}, t_{j, i}^{(M)}\}_{i=1}^n$ occurs when $i = m$,
- (4) time delay $T_{s_l}(\pi/2\lambda_{m-1}) - \varepsilon$, where ε is a small positive quantity and, $T_{s_l}\lambda_m > \pi/2$,
- (5) $(\lambda_{\max}/\lambda_{m-1}) \leq 3$, and
- (6) $K_1 > K_2/\lambda_{\min}^2$ or $K_1 < K_2/\lambda_{\max}^2$,

it is possible to stabilize an undamped (open loop) system for small gains.

Result 2.12

For the undamped system described in Result 2.11, velocity feedback control will be stable as long as $\mu < G$, where G is the minimum of all positive B_l , for $l = 0, 1, 2, \dots$, where

$$B_l = \frac{-1}{a_{s_l} K_1 \eta_l \sin(\eta_l T_{s_l}) \sum_{i=1}^n (t_{s_l, i}^{(M)} t_{j, i}^{(M)}) / (\lambda_i^2 - \eta_l^2)} \quad \text{and} \quad \eta_l = \frac{(2l + 1)\pi}{2T_{s_l}}$$

2.3. Underdamped systems

This section deals with underdamped systems. Specializing Equation (9) to underdamped systems, and utilizing Result 2.2 we get the following result which is again applicable to the case when only system poles are considered.

Result 2.13

When using PID control for underdamped systems, $\xi_i < \lambda_i$, $i = 1, 2, \dots, n$, a sufficient condition for the closed loop system to be stable for small gains is

$$-\frac{1}{(\lambda_r^2 - \xi_r^2)^{1/2}} \left[K_0 - \left(K_1 + \frac{K_2}{\lambda_r^2} \right) \xi_r \right] \left(\sum_{k=1}^p a_{s_k} \exp[\xi_r T_{s_k}] \sin((\lambda_r^2 - \xi_r^2)^{1/2} T_{s_k}) t_{s_k, r}^{(M)} t_{j, r}^{(M)} \right) + \left[K_1 - \frac{K_2}{\lambda_r^2} \right] \left(\sum_{k=1}^p a_{s_k} \exp[\xi_r T_{s_k}] \cos((\lambda_r^2 - \xi_r^2)^{1/2} T_{s_k}) t_{s_k, r}^{(M)} t_{j, r}^{(M)} \right) > 0$$

for $r = 1, 2, \dots, n$.

Result 2.14

When the sensor and actuator are collocated and only one sensor is used, for PID control, if $(K_1 - K_2/\lambda_r^2) \neq 0$, for all r , a sufficient condition for small gains stability is

$$a_j \left[K_1 - \frac{K_2}{\lambda_r^2} \right] \cos((\lambda_r^2 - \xi_r^2)^{1/2} T_{s_k} + \phi) > 0 \quad \text{for } r = 1, 2, \dots, n$$

where

$$\pi = \tan^{-1} \left[\frac{K_0 - (K_1 + (K_2/\lambda_r^2)) \xi_r}{(K_1 - (K_2/\lambda_r^2)) (\lambda_r^2 - \xi_r^2)^{1/2}} \right]$$

Result 2.15

When using one sensor, collocation of the sensor with an actuator of the given feedback control type will cause the closed loop system poles to move to the left in the s -plane, as long as the given condition on the time delay is satisfied.

(a) For velocity feedback, the time delay needs to satisfy

$$T_j < \min_{\forall r} \left[\frac{(\pi/2) + \phi}{(\lambda_r^2 - \xi_r^2)^{1/2}} \right]$$

where

$$\phi = \tan^{-1} \left[\frac{\xi_r}{(\lambda_r^2 - \xi_r^2)^{1/2}} \right]$$

(b) For integral feedback, the time delay needs to satisfy

$$T_j < \min_{\forall r} \left[\frac{(\pi/2) - \phi}{(\lambda_r^2 - \xi_r^2)^{1/2}} \right]$$

where ϕ is as in part (a).

(c) For proportional feedback, the time delay needs to satisfy

$$0 < T_j < \min_{\forall r} \left[\frac{\pi}{(\lambda_r^2 - \xi_r^2)^{1/2}} \right]$$

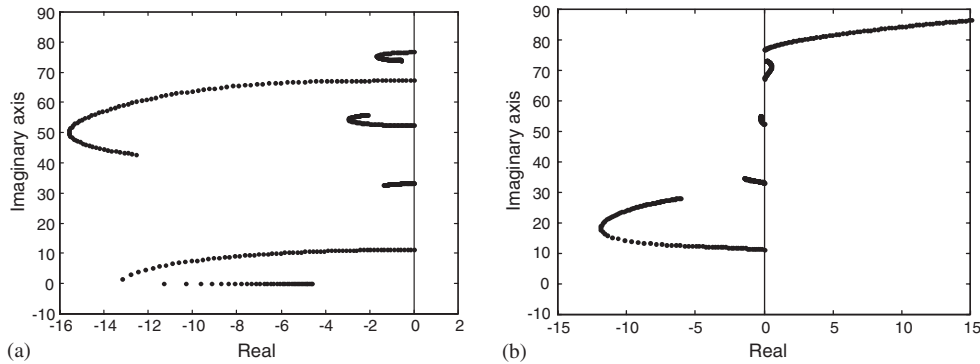


Figure 2. Root loci of closed loop system poles for collocated velocity feedback control with $j=4$, $s_1=4$, $a_4=1$, and time delay (a) $T_4=0$ s, (b) $T_4=0.025$ s.

(d) For a PID controller, the time delay needs to satisfy

$$T_j < \min_{v_r} \left[\frac{(\pi/2) - \phi}{(\lambda_r^2 - \zeta_r^2)^{1/2}} \right]$$

where ϕ is as defined in Result 2.14, when $K_1 > K_2/\lambda_{\min}^2$ and $a_j > 0$, or $K_1 < K_2/\lambda_{\max}^2$ and $a_j < 0$.

2.4. Numerical results

The numerical results are obtained for an undamped shear frame building structure (five-degree-of-freedom system) shown in Figure 1. The mass and the stiffness of each storey are 1 and 1600 (taken in SI units), respectively. The root loci presented only show the system poles. The controller’s gain μ has been varied from 0 to 100 units. Velocity feedback control is used for all the results.

The first example deals with the collocated control of the structure with and without time delay. The controller and the sensor are collocated at the fourth storey. Figure 2(a) shows the root loci of the closed loop system poles for velocity feedback control with no time delay ($T_4=0$ s). As expected from Result 2.6, the system is stable since the system’s closed loop poles have negative real parts. Figure 2(b) shows the root loci for the closed loop system poles with velocity feedback control when a time delay of $T_4=0.025$ s is used. Introducing a time delay of $T_4=0.025$ s makes the system unstable even for very small gains, as predicted by Result 2.4.

In the second example, the non-collocated control of the structure is studied with and without time delay. The actuator is placed at mass 4 (fourth storey) and is fed the velocity signal from location 5 (fifth storey). Figure 3(a) shows the root loci for the closed loop system poles for velocity feedback control with no time delay ($T_5=0$ s) and $j=4$, $s_1=5$, $a_5=1$. As guaranteed by Result 2.8, even for vanishingly small gains, the third, fourth, and fifth closed loop system poles are in the right-half s -plane, hence causing instability. However, the introduction of an appropriate time delay, such as $T_5=0.04$ s makes the closed loop system

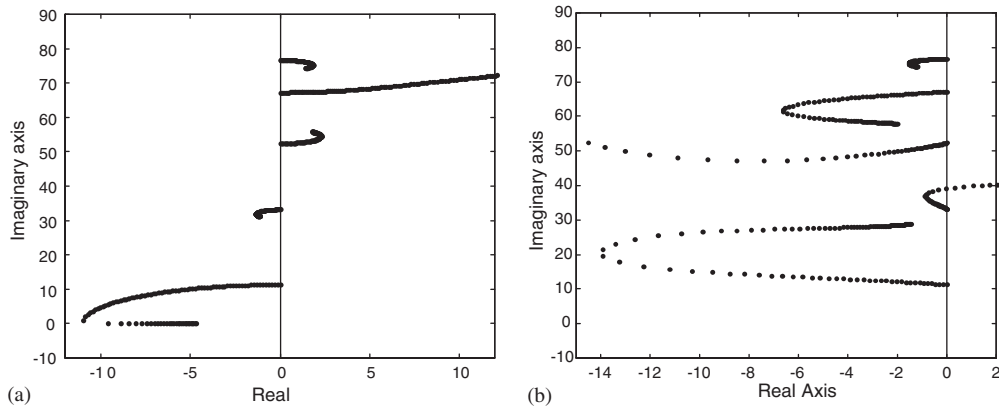


Figure 3. Root loci of closed loop system poles for non-collocated velocity feedback control with $j=4$, $s_1=5$, $a_5=1$, and time delay (a) $T_5=0$ s, (b) $T_5=0.04$ s.

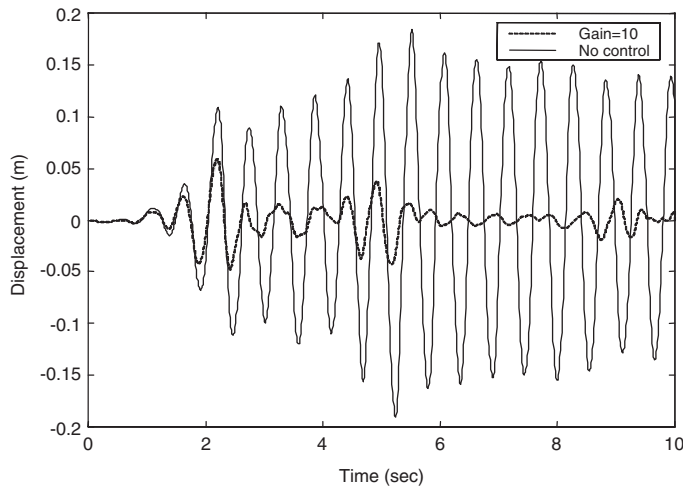


Figure 4. Relative displacement response of mass 5 ($j=4$, $s_1=5$, $a_5=1$, and $T_5=0.04$ s) for non-collocated velocity control.

poles remain in the left-half plane until a certain value of the controller gain. This is illustrated in Figure 3(b), where the closed loop system poles are shown for $j=4$, $s_1=5$, $a_5=1$, and a time delay of $T_5=0.04$ s. The upper bound on the gain for stability obtained by tracing the root loci is the same as the one predicted by Result 2.12. This example shows that by appropriately injecting time delay into a system, it is possible to stabilize a system which is unstable for zero time delay.

Figure 4 shows the displacement time history of mass 5 relative to the base, when the structure is subjected to the ground motion of the S00E component of the Imperial Valley Earthquake of 1940. The structural responses are numerically computed using a fourth-order

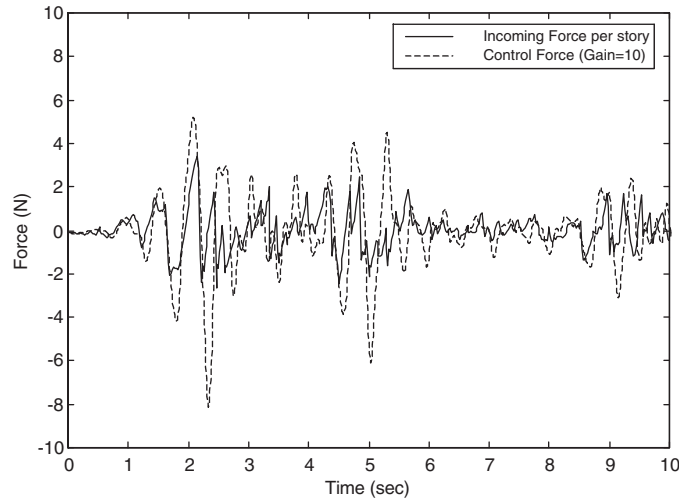


Figure 5. Incoming force per storey and control force time histories ($j=4$, $s_1=5$, $a_5=1$, and $T_5=0.04$ s) for non-collocated velocity control.

Runge–Kutta scheme. The response time histories are shown only for the first 10 s. The response is shown for no control ($\mu=0$), and for $\mu=10$ units, using non-collocated velocity control with $j=4$, $s_1=5$, $a_5=1$, and $T_5=0.04$ s. The results on Figure 4 show that by using intentional time-delayed velocity feedback, the displacement of the 5th mass is significantly smaller than the displacement of the mass when no control is used. Figure 5 shows the time histories of the incoming force per storey (i.e. negative of storey mass times ground acceleration) and the control force required when the controller's gain is $\mu=10$ units.

To explore the robustness of this control methodology, numerical results of the sensitivity of the closed loop system poles to changes in the mass, stiffness and time delay parameters (for the nominal system presented in the last example) are presented in the next section.

2.5. Sensitivity of the stability to perturbed parameters

There is always uncertainty about the exact values of the system's parameters. The uncertainty might come from not being able to measure or estimate the system parameters accurately. It may also come from variations of the system parameters caused by fatigue, structural degradation, etc. Changes in the parameter values will lead to changes in the closed loop poles, and thus changes in the performance of the system. This stresses the importance of knowing how sensitive the time-delayed control is to parameter variations. Furthermore, we have shown that the purposeful injection of time delays in non-collocated systems brings about stability. As the injection of such time delays in actual systems can at best be chosen only approximately (because of the uncertainties in actuator dynamics, etc.) it is important to examine the sensitivity of such a control technique to uncertainties in the time delays.

These sensitivities are studied for the undamped shear frame building structure described in Section 2.4 (see Figure 1). The results are for the non-collocated velocity feedback control, where the actuator is placed at mass 4, and the sensor takes delayed velocity readings from

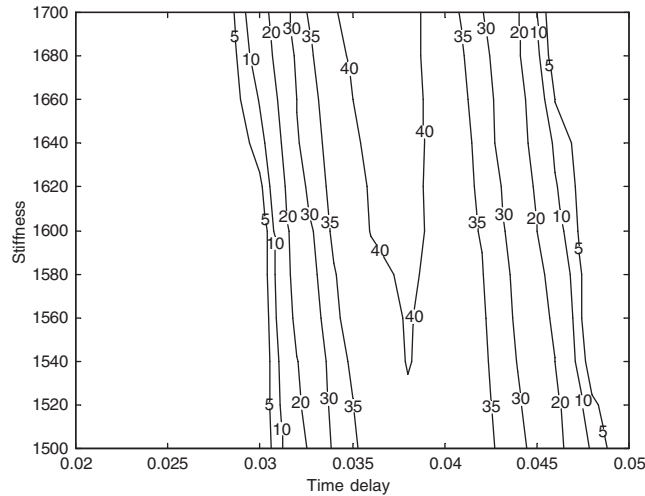


Figure 6. Sensitivity of the maximum gain for stability to changes in stiffness and time delay for $j=4$, $s_1=5$, $a_5=1$, and mass = 1.

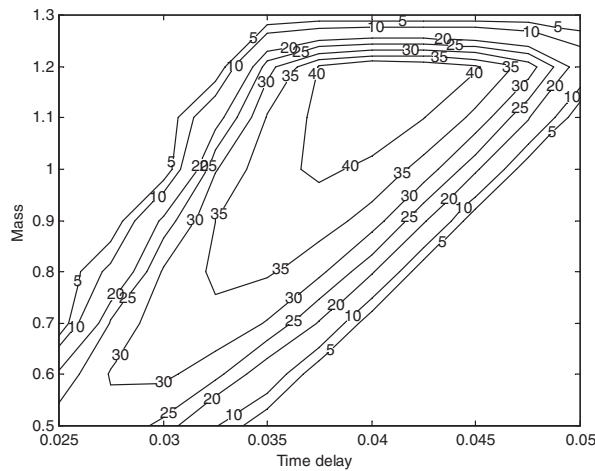


Figure 7. Sensitivity of the maximum gain for stability to changes in mass and time delay for $j=4$, $s_1=5$, $a_5=1$, and stiffness = 1600.

mass 5 ($j=4$, $s_1=5$, $a_5=1$). By varying the stiffness (or mass) and the time delay parameters of the shear frame structure, the changes of the maximum gain for stability of the system are obtained. The maximum gain for stability is numerically computed, and it is the largest gain that assures stability when closed loop system poles are considered. The results are presented through contour maps with constant gain curves.

Level curves of maximum gain for stability for the above described system are presented in Figures 6 and 7. In Figure 6 the stiffness and the time delay are varied, keeping the mass

constant at 1 (SI units). Sensitivity to variations of the mass and the time delay are presented on Figure 7, when the stiffness is kept constant at 1600 (SI units).

Both graphs show a continuous dependence of the maximum gain for stability on the chosen parameters. The figures show that stable dislocated control brought about by the purposeful injection of time delays could be made effective even in the presence of considerable uncertainties in the parameters that model the structural system. Further results on the stability of controlled systems with uncertainties in the system parameters and time delay are presented in Section 5. The next section deals with the control of more general linear systems which include both non-classically and classically damped structures.

3. NON-CLASSICALLY DAMPED SYSTEMS

In the last section we presented results dealing with classically damped systems, where several of the results apply when only system poles are considered. In this section we present a formulation that deals with more general systems, and the results apply to both, non-classically damped as well as to classically damped systems. Furthermore, the results apply when all the poles are considered; they are not just limited to considering system poles. The importance of having a formulation that deals with ‘all’ the poles of the control system with time delays will be illustrated in Section 4 where it is shown that a pole not originating from an open loop pole dictates the stability of the system.

We show that when all the open loop poles have negative real parts and the controller transfer function is an analytic function, then given any time delays there exists a range in the gain (which could depend on the time delays) for which the closed loop feedback system is stable. The results are then specialized to systems with a single sensor. We show that under some conditions there exists a range in the gain for which the closed loop system is stable for all time delays. The section ends with the application of some of the results to a single degree of freedom oscillator.

3.1. General formulation

The same general formulation given for classically damped systems (Section 2) will be used in this section, except that the systems considered here are more general (also see von Bremen and Udvardia [14]). They include both classically damped and non-classically damped systems. Consider the following matrix equation corresponding to a structural system with the response $x(t)$ given as

$$Mx'' + Cx' + Kx = g(t), \quad x(0) = 0 \text{ and } x'(0) = 0 \quad (14)$$

where M is an n by n mass matrix, C is the $n \times n$ damping matrix and K is the $n \times n$ stiffness matrix. The n -vector $g(t)$ is the distributed applied force. The Laplace transform of the above system is

$$\tilde{A}(s)\tilde{x}(s) = (Ms^2 + Cs + K)\tilde{x}(s) = \tilde{g}(s) \quad (15)$$

As in Section 2, we use p responses in the feedback control. A linear combination of the sensed responses are fed to the controller which generates the control force. In general, the system may have several actuators; in this paper we will deal with one actuator. Suppose we have a control effort affecting the j th equation of Equation (15) given by $\mu(f(s), \tilde{x}(s))e_j$, where $(f(s), \tilde{x}(s)) = \sum_{i=1}^n f_i(s)\tilde{x}_i(s)$, e_j is a vector with 1 in the j th location and zero for all other entries, and μ is the control gain. The function $f_i(s)$ contains the controller transfer function which uses the signal from $\tilde{x}_i(s)$, and in the presence of a time delay T_i , it includes the term $\exp[-sT_i]$ as a factor. Equation (15) with the control effort becomes

$$\tilde{A}(s)\tilde{x}(s) = \tilde{g}(s) - \mu(f(s), \tilde{x}(s))e_j \quad (16)$$

Moving the term $\mu(f(s), \tilde{x}(s))e_j$ to the left-hand side of (16), we get the equation

$$\tilde{A}_1(s)\tilde{x}(s) = \tilde{g}(s) \quad (17)$$

The open loop poles of Equation (17) are given by Equation (18a) and the closed loop poles are given by Equation (18b) as follows:

$$\det[\tilde{A}(s)] = 0 \quad (18a)$$

$$\det[\tilde{A}_1(s)] = 0 \quad (18b)$$

The equation for the closed loop poles can be written as

$$\det[\tilde{A}_1(s)] = \det[\tilde{A}(s)] + \mu \sum_{i=1}^n f_i(s)\tilde{A}_{ij}(s) \quad (19)$$

where $\tilde{A}_{ij}(s)$ is the cofactor of $\tilde{a}_{ij}(s)$, in other words $\tilde{A}_{ij}(s) = (-1)^{(i+j)}\{\text{Minor}(\tilde{a}_{ij}(s))\}$, and the matrix \tilde{A} is the one defined in Equation (15).

3.2. General analytical results

The stability of the system described in Equation (16) is dictated by the sign of the real part of the closed loop poles. Using the argument principle, we can determine bounds on the gain so that the system described in Equation (16) is stable in the presence of time delays, provided the open loop poles of the system have negative real parts.

The next result is similar to Result 2.1. It gives conditions so that the open and closed loop systems have no poles in common.

Result 3.1

Suppose the open loop poles are given by λ_k , with $k = 1, 2, \dots, 2n$ and the condition

$$q(\lambda_k) = \sum_{i=1}^n f_i(\lambda_k)\tilde{A}_{ij}(\lambda_k) \neq 0 \quad \text{for } k = 1, 2, \dots, 2n$$

is satisfied. Then the closed loop system and the open loop system have no poles in common.

Proof

For any k , clearly

$$\begin{aligned}\det[\tilde{A}_1(\lambda_k)] &= \det[\tilde{A}_1(\lambda_k)] + \mu \sum_{i=1}^n f_i(\lambda_k) \tilde{A}_{ij}(\lambda_k) \\ &= \mu \sum_{i=1}^n f_i(\lambda_k) \tilde{A}_{ij}(\lambda_k) \neq 0\end{aligned}$$

So no solution of Equation (18a) is shared by Equation (19), establishing the claim.

For the stability of the closed loop system, we need the real part of the closed loop poles to be negative. The next result gives bounds on the gain so that the closed loop system remains stable.

Result 3.2

For any given set of time delays, suppose the open loop poles $\lambda_1, \lambda_2, \dots, \lambda_{2n}$ all have negative real parts and the following two conditions are satisfied:

- (a) $q(s) = \sum_{i=1}^n f_i(s) \tilde{A}_{ij}(s) \neq 0$, and
- (b) $q(s)$ is analytic,

for all s in the right-half complex plane and along the imaginary axis. Then there exists an interval $I_{\mu^*} = [-\mu^*, \mu^*]$, with $\mu^* > 0$, such that for any gain $\mu \in I_{\mu^*}$, the closed loop poles are in the left-half complex plane (i.e., the system is stable).

Proof

We will use the argument principle (see pp. 152–154 in Ahlfors [15]). Equation (19) can be visualized as

$$\det[\tilde{A}_1(s)] = h(s) = p(s) + \mu q(s)$$

where $p(s) = \det[\tilde{A}(s)]$, and $q(s)$ is as above. Consider the contour given by the half-circle of radius R in the right-half plane with boundary Γ_R and enclosing the region Ω_R , see Figure 8.

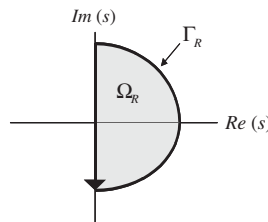


Figure 8. Contour of integration.

For any fixed R we have

$$\frac{h'(s)}{h(s)} = \frac{p'(s) + \mu q'(s)}{p(s) + \mu q(s)} = \frac{p'(s) + \mu q'(s)}{p(s)(1 + (\mu q(s)/p(s)))}$$

Now

$$\frac{1}{1 + (\mu q(s)/p(s))} = \sum_{k=0}^{\infty} \left(-\frac{\mu q(s)}{p(s)} \right)^k \quad \text{for all } s \in \Omega_R, \text{ provided}$$

$$\left| \frac{\mu q(s)}{p(s)} \right| < 1 \quad \text{or} \quad |\mu| < \left| \frac{p(s)}{q(s)} \right|$$

By conditions (a) and (b), and the fact that $p(s)$ is a polynomial, we have that $p(s)/q(s)$ is analytic on Ω_R ; also, $p(s) \neq 0$ in Ω_R . Thus by the minimum modulus principle, $|p(s)/q(s)|$ has a non-zero minimum on the boundary Γ_R of Ω_R . Let μ^* be such that

$$\mu^* < \min_{s \in \Omega_R} \left| \frac{p(s)}{q(s)} \right| = \min_{s \in \Gamma_R} \left| \frac{p(s)}{q(s)} \right|$$

Therefore, for any $\mu \in [-\mu^*, \mu^*]$, the infinite series converges. Let $\mu \in [-\mu^*, \mu^*]$, we then have

$$\begin{aligned} \int_{\Gamma_R} \frac{h'(s)}{h(s)} ds &= \int_{\Gamma_R} \frac{p'(s) + \mu q'(s)}{p(s)} \left(\sum_{k=0}^{\infty} \left(-\frac{\mu q(s)}{p(s)} \right)^k \right) ds \\ &= \sum_{k=0}^{\infty} \left(\int_{\Gamma_R} \frac{p'(s) + \mu q'(s)}{p(s)} \left(-\frac{\mu q(s)}{p(s)} \right)^k ds \right) = 0 \end{aligned}$$

Note that for each k , the integral is an integral of an analytic function over a closed curve, and thus equal to zero. R is arbitrary, so by the argument principle (see pp. 152–154 in Ahlfors [15]) there exists a range $[-\mu^*, \mu^*]$ in μ for which all the closed loop poles are in the left-half plane.

Result 3.2 can be strengthened so that condition (a) is not needed. That is, the function $q(s)$ is allowed to have zeros in the right-half plane.

Result 3.3

For a given set of time delays, suppose the open loop poles $\lambda_1, \lambda_2, \dots, \lambda_{2n}$ all have negative real parts, the function $q(s)$ is analytic for all s in the right-half complex plane and along the imaginary axis, and $q(s)$ has zeros at s_1, s_2, \dots, s_m in the right-half complex plane (including perhaps zeros on the imaginary axis). Then there exists an interval $I_{\mu^*} = [-\mu^*, \mu^*]$, with $\mu^* > 0$, such that for any gain $\mu \in I_{\mu^*}$ the closed loop poles are in the left-half complex plane (i.e. the system is stable).

Proof

The proof is similar to the one given for Result 3.2. First suppose that $q(s)$ has only one zero s_1 in the right-half complex plane.

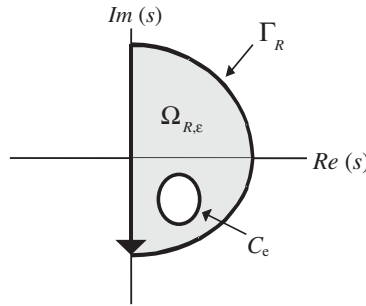


Figure 9. Contour of integration.

Let $\Gamma_{R,\epsilon}$ be the contour given by $\Gamma_{R,\epsilon} = \Gamma_R \cup C_\epsilon$, where Γ_R is the contour given by the half circle of radius R in the right-half plane, and C_ϵ is the circle of radius ϵ centered about s_1 . Let $\Omega_{R,\epsilon}$ be the region bounded by the circle C_ϵ and the half circle Γ_R , see Figure 9.

As in the proof of Result 3.2, $\det[\tilde{\mathbf{A}}_1(s)] = h(s) = p(s) + \mu q(s)$. We need to show that

$$\frac{1}{1 + (\mu q(s)/p(s))} = \sum_{k=0}^{\infty} \left(-\frac{\mu q(s)}{p(s)} \right)^k$$

converges for $\mu \in [-\mu^*, \mu^*]$, where μ^* needs to be determined. In the region $\Omega_{R,\epsilon}$, the function $p(s)/q(s)$ is analytic, and thus $|p(s)/q(s)|$ has a minimum on the boundary $\Gamma_{R,\epsilon}$ of $\Omega_{R,\epsilon}$ (recall that p has no zeros in the left-half plane, nor on the imaginary axis). The question is, what will occur when $\epsilon \rightarrow 0$? Since the minimum occurs on the boundary $\Gamma_{R,\epsilon}$, it must either occur on Γ_R or on C_ϵ . It will be shown that it must occur on Γ_R .

The function $q(s)$ can be expressed as $q(s) = (s - s_1)g(s)$. The function $p(s)/g(s)$ is analytic inside the closed disk bounded by C_ϵ , so it has a non-zero minimum $M_\epsilon = \min_{s \in C_\epsilon} |p(s)/g(s)|$. Using the last observations we get

$$\min_{s \in C_\epsilon} \left| \frac{p(s)}{q(s)} \right| = \min_{s \in C_\epsilon} \left| \frac{p(s)}{(s - s_1)g(s)} \right| \geq \min_{s \in C_\epsilon} \left| \frac{p(s)}{g(s)} \right| \min_{s \in C_\epsilon} \frac{1}{|s - s_1|} = M_\epsilon \frac{1}{\epsilon}$$

Thus, if $\epsilon \rightarrow 0$, then $\min_{s \in C_\epsilon} |p(s)/q(s)| \rightarrow \infty$. Therefore, the minimum of $|p(s)/q(s)|$ over the region $\Omega_{R,\epsilon}$ must occur on the boundary Γ_R . Using the fact the minimum occurs on Γ_R , we see that the series

$$\frac{1}{1 + (\mu q(s)/p(s))} = \sum_{k=0}^{\infty} \left(-\frac{\mu q(s)}{p(s)} \right)^k$$

converges. We can apply exactly the same argument given in the proof of Result 3.2, establishing the result.

When $q(s)$ has more than one zero (even repeated zeros), a similar argument as the one presented can be used to show that the minimum will occur on the boundary Γ_R , and hence the series

$$\frac{1}{1 + (\mu q(s)/p(s))} = \sum_{k=0}^{\infty} \left(-\frac{\mu q(s)}{p(s)} \right)^k$$

converges, and again the result follows.

Note that Results 3.2 and 3.3 apply for systems with time delay, and the function $q(s)$ would contain all the expressions containing time delay.

3.3. Results for one actuator and one sensor

In this section we present results that apply to the system described in Equation (16), when one sensor and one actuator are used.

Since we have one sensor at the i th location and the actuator at the j th location, then the closed loop poles are given by

$$\begin{aligned}\det[\tilde{A}_1(s)] &= \det[\tilde{A}(s)] + \mu f_i(s)\tilde{A}_{ij}(s) \\ &= p(s) + \mu q(s)\end{aligned}\quad (20)$$

Here $q(s) = f_i(s)\tilde{A}_{ij}(s)$, and $p(s) = \det[\tilde{A}(s)]$. The function $f_i(s)$ is the product of the controller transfer function $\tau_c(s)$ and the term $\exp[-sT_i]$ due to the time delay. Let $g(s) = \tau_c(s)\tilde{A}_{ij}(s)$, then $q(s) = g(s)\exp[-sT_i]$. Since \tilde{A}_{ij} is a polynomial, it is analytic, and if we assume that the controller transfer function $\tau_c(s)$ is analytic in the right-half plane, then $g(s)$ is analytic in the right-half plane. In most situations it is reasonable to expect that $p(s)$ goes to infinity faster than $q(s)$ does as $|s| \rightarrow \infty$, so here we shall assume that $|p(s)/q(s)| \rightarrow \infty$ as $|s| \rightarrow \infty$.

Assuming that the open loop poles have negative real parts, then Result 3.3 applies. Following the proof of the result, for large enough R , the bound on the gain for stability is given by

$$\mu^* < \min_{s \in \Omega_R} \left| \frac{p(s)}{q(s)} \right| = \min_{s \in \Gamma_R} \left| \frac{p(s)}{q(s)} \right|$$

The boundary Γ_R is composed of a semicircle C_R of radius R and a segment of the imaginary axis I_R of length $2R$. The minimum must occur on the segment I_R , provided R is large enough and $|p(s)/q(s)| \rightarrow \infty$ as $|s| \rightarrow \infty$. Since $|p(s)/q(s)| \rightarrow \infty$ as $|s| \rightarrow \infty$, then there exists an R^* so that the minimum occurs for this R^* , and for any $R^* < R$ we have $\min_{s \in \Omega_{R^*}} |p(s)/q(s)| = \min_{s \in \Omega_R} |p(s)/q(s)|$. For $R^* < R$, C_{R^*} is inside Ω_R , by the minimum modulus principle, the minimum cannot occur in the interior of Ω_R , thus it occurs on I_{R^*} . The above observations are used in the proof of the following result.

Result 3.4

When using one sensor and one actuator, there exists an interval $[-\mu^*, \mu^*]$ in the gain μ , with $\mu^* > 0$, which is *independent of time delay*, such that the closed loop poles have negative real parts, provided all the open loop poles have negative real parts, and $|p(s)/q(s)| \rightarrow \infty$ as $|s| \rightarrow \infty$.

Proof

By the previous argument, for large enough R , the minimum $\min_{s \in \Gamma_R} |p(s)/q(s)|$ will occur on I_R . Say it occurs at $s = w^{**}j$ ($j = \sqrt{-1}$), then for large enough R ,

$$\mu^* < \mu^{**} = \min_{s \in \Omega_R} \left| \frac{p(s)}{q(s)} \right| = \min_{w \in I_R} \left| \frac{p(wj)}{g(wj)\exp[-jwT_i]} \right| = \min_{w \in I_R} \left| \frac{p(wj)}{g(wj)} \right| = \left| \frac{p(w^{**}j)}{g(w^{**}j)} \right| \quad (21)$$

This establishes the result.

From the result, the bound μ^{**} can be obtained by considering the system with no time delay and finding the minimum of $|p(wj)/q(wj)|$ for $w \in I_R$. For some systems it may be possible that μ^{**} is actually the maximum gain for stability for the system with no time delay. This will be the case in *Example 1* shown after Result 3.6 as well as for the control systems explored in Section 4. That is, for zero time delay one finds the maximum gain for stability using positive and negative feedback, and μ^{**} is the minimum of the two maximum gains. In general, however, it is not necessarily true that the minimum of the maximum gains for stability μ^{**} is achieved for the system with zero time delay. It is possible for some systems that the maximum gain for stability of the system with zero time delay is larger than the gain that is independent of time delay. This case will be illustrated in *Example 2*.

Since the bound μ^{**} occurs on the imaginary axis and it may not necessarily be the bound for the maximum gain for stability for the system with no time delay, and it is a bound on the gain for which the system is stable for all time delays, one might ask if μ^{**} will actually be the maximum gain for stability at some time delay. The following result answers this question.

Result 3.5

For systems with one sensor and one actuator, as described in Result 3.4, suppose μ^{**} occurs at $s = w^{**}j$, then there exists a time delay T such that

$$p(w^{**}j) + \mu^{**} q(w^{**}j) e^{-w^{**}Tj} = 0.$$

That is, the bound of the maximum gain for stability independent of time delay given in Result 3.4 is achieved at some time delay T . The value of T will be given in the proof and it is derived from the system properties without time delay.

Proof

Let the real and imaginary parts of $p(w^{**}j)$ and $q(w^{**}j)$ from Result 3.4 be given by

$$p(w^{**}j) = p_R + p_I j \quad \text{and} \quad q(w^{**}j) = g_R + g_I j \quad (22)$$

Consider

$$p_R + p_I j + \mu^{**} (g_R + g_I j)(x - yj) = 0$$

Then

$$x - yj = -\frac{p_R g_R + p_I g_I}{\mu^{**} (g_R^2 + g_I^2)} - \frac{p_I g_R - p_R g_I}{\mu^{**} (g_R^2 + g_I^2)} \quad (23)$$

Note that $\mu^{**} = \sqrt{(p_R^2 + p_I^2)/(g_R^2 + g_I^2)}$ and $x^2 + y^2 = 1$. Therefore we can take $\cos(w^{**}T) = x$ and $\sin(w^{**}T) = y$, establishing the result.

Result 3.5 indicates that there is a time delay at which the system will achieve the bound on the maximum gain for stability given in Result 3.4. The result also indicates if the bound of the maximum gain for stability that is independent of time delay is actually achieved or not for zero time delay. If $x = 1$, then for the system with zero time delay the maximum gain for stability will be reached with gain $\mu = \mu^{**}$. Similarly, if $x = -1$, then for the system with zero time delay the maximum gain for stability will be reached with gain $\mu = -\mu^{**}$. If $|x| \neq 1$, then the maximum gain for stability of the system with zero time delay is larger than the

maximum gain for stability that is independent of time delay. The question of the uniqueness of the occurrence of poles at a gain of μ^{**} (for positive and negative feedback) is dealt with in the next result.

Result 3.6

For the case of a single actuator and a single sensor, suppose that a closed loop pole given by (20) is at $s = w^*j$, $\mu = \mu^*$, and with a time delay of $T = T^*$. Then there exist closed loop poles at $s = w^*j$, $\mu = -\mu^*$, with time delays $T = T^* + ((2n + 1)\pi/w^*)$, for $n = 0, 1, 2, \dots$, and at $s = w^*j$, $\mu = \mu^*$, with time delays $T = T^* + 2n\pi/w^*$, for $n = 1, 2, \dots$.

Proof

For a pole on the imaginary axis, we have

$$p(wj) + \mu g(wj) \exp[-jwT] = p(wj) + \mu g(wj)(\cos(wT) - j \sin(wT)) = 0 \quad (24)$$

When the pole occurs at $w = w^*$, $\mu = \mu^*$, and $T = T^*$, then Equation (24) is also satisfied with $w = w^*$, provided the time delay T satisfies the equations

$$\cos(w^*T^*) = \cos(w^*T) \quad \text{and} \quad \sin(w^*T^*) = \sin(w^*T)$$

These equations are satisfied when $T = T^* + (2n\pi/w^*)$, for $n = 1, 2, \dots$. Similarly, when the pole occurs at $w = w^*$, $\mu = \mu^*$, and $T = T^*$, then Equation (24) is also satisfied with $w = w^*$, $\mu = -\mu^*$, provided the time delay T satisfies the equations

$$\cos(w^*T^*) = -\cos(w^*T) \quad \text{and} \quad \sin(w^*T^*) = -\sin(w^*T)$$

And these equations are satisfied if $T = T^* + ((2n + 1)\pi/w^*)$, for $n = 0, 1, 2, \dots$.

One consequence of this result is that the maximum gain for stability which is independent of time delay (from Result 3.4) will be achieved for both positive and negative feedback, when an appropriate time delay is chosen. A time delay T^* at which the minimum value of the maximum gain for stability is achieved can be obtained using Result 3.6.

In the next example, the bound on the maximum gain for stability that is independent of time delay (given in Results 3.4) coincides with the maximum gain for stability of the system with zero time delay.

Example 1

As a simple illustration of Results 3.4–3.6, consider a single degree of freedom oscillator with response $x(t)$, and with mass m , damping $c > 0$, and stiffness $k > 0$. The oscillator is controlled by using a time-delayed negative velocity feedback $-\mu x'(t - T)$, with time delay T , and using a control gain μ . The motion of the oscillator is described by the scalar differential equation

$$mx''(t) + cx'(t) + kx(t) = -\mu x'(t - T), \quad x(0) = 0, \quad x'(0) = 0 \quad (25)$$

The Laplace transform of Equation (25) is

$$(ms^2 + cs + k + \mu s \exp[-sT])\tilde{x}(s) = 0 \quad (26)$$

The closed loop poles of the system described by Equation (25) are the zeros of the equation

$$ms^2 + cs + k + \mu s \exp[-sT] = 0 \quad (27)$$

From Result 3.4, we have that the maximum gain for stability which is independent of time delay occurs on the imaginary axis at some $s = jw$. Evaluation of Equation (27) at $s = jw$ gives

$$-mw^2 + cwj + k + j\mu w(\cos(wT) + j \sin(wT)) = 0 \quad (28)$$

The imaginary part of Equation (28) is

$$cw + \mu w(\cos(wT)) = 0 \quad \text{or} \quad \cos(wT) = \frac{-c}{\mu} \quad (29)$$

Note that $w = 0$ is not a solution, since it would violate Equation (28). Equation (29) has a solution only if $|c/\mu| \leq 1$, that is $|\mu| \geq c$. Thus for $|\mu| < c$, Equation (28) has all poles in the left-half complex plane (i.e. all solutions have negative real parts).

For zero time delay ($T = 0$) the closed loop poles are given by the zeros of the equation $ms^2 + (c + \mu)s + k = 0$. From the Routh stability criterion, for negative feedback ($\mu > 0$) the system will be stable for all gains. On the other hand, for positive feedback ($\mu < 0$), the system has a cross-over pole at $\mu = -c$ and $w = \sqrt{k/m}$.

Using Result 3.5 one can confirm this observation. From Result 3.5 we have

$$\mu^{**} = \min_{w \in I_R} \left| \frac{p(wj)}{g(wj)} \right| = \min_{w \in I_R} \left| \frac{-mw^2 + k + cwj}{wj} \right| = c$$

and the minimum occurs at $w^{**} = \sqrt{k/m}$.

Additionally from Result 3.5, for negative feedback we have that $x = \cos(\sqrt{k/m}T) = -1$ and $y = \sin(\sqrt{k/m}T) = 0$. The smallest time delay for which these equations are satisfied is $T = \pi\sqrt{m/k}$. Thus for negative feedback and zero time delay the bound on the maximum gain for stability independent of time delay is not achieved. For positive feedback we have $x = \cos(\sqrt{k/m}T) = 1$ and $y = \sin(\sqrt{k/m}T) = 0$, and thus the bound on the maximum gain for stability is reached at zero time delay.

Using result 3.6 we have that for negative feedback the system will reach the minimum bound for the gain for stability at $w = \sqrt{k/m}$ for the time delays $T = (2n + 1)\pi\sqrt{m/k}$ (for $n = 0, 1, 2, \dots$) with a gain of $\mu = c$. For positive feedback the system will reach the minimum bound for the gain at $w = \sqrt{k/m}$ for the time delays $T = 2n\pi\sqrt{m/k}$ (for $n = 0, 1, 2, \dots$) with a gain of $\mu = -c$.

The next example shows the case where the maximum gain for stability of the system with zero time delay is larger than the gain for stability that is independent of time delay, given in Result 3.4.

Example 2

Consider again a single degree of freedom oscillator with response $x(t)$, and with mass m , damping $c > 0$, and stiffness $k > 0$. This time the oscillator is controlled by using the negative feedback time-delayed proportional control $-\mu x(t - T)$, with time delay T , and a control gain μ . The motion of the oscillator is described by the scalar differential equation

$$mx''(t) + cx'(t) + kx(t) = -\mu x(t - T), \quad x(0) = 0 \quad \text{and} \quad x'(0) = 0 \quad (30)$$

After taking the Laplace transform of (30), the poles of the system are the zeros of the equation

$$ms^2 + cs + k + \mu \exp[-sT] = 0 \quad (31)$$

The bound on the maximum gain for stability that is independent of time delay can be obtained using Equation (21). When $2mk - c^2 > 0$, we have

$$\mu^{**} = \min_{w \in I_R} \left| \frac{p(wj)}{g(wj)} \right| = \min_{w \in I_R} | -mw^2 + cwj + k | = \sqrt{\frac{c^2(4mk - c^2)}{4m^2}} \quad (32)$$

Where the minimum in Equation (32) occurs at $w^{**} = \sqrt{(2mk - c^2)/2m^2}$.

For zero time delay the closed loop poles are the zeros of the equation $ms^2 + cs + (k + \mu) = 0$. Based on the Routh stability criterion, the negative feedback system will be stable for all gains. In the case of positive feedback, the system will have a unique cross-over at $w=0$ and a gain of $\mu = -k$. When $2mk - c^2 > 0$ we have that $\mu^{**} < k$. This indicates that the magnitude of the maximum gain for stability of the system with zero time delay for positive feedback is larger than the bound of the gain that is independent of time delay.

The values for x and y in Equation (23) are

$$x = -\frac{c}{\sqrt{4km - c^2}} \quad \text{and} \quad y = \sqrt{\frac{4km - 2c^2}{4km - c^2}} \quad (33)$$

From Result 3.5 one can compute the time delay at which the bound on the gain for stability that is independent of time delay is reached by the system. The smallest time delay at which the system reaches the bound on the gain for stability that is independent of time delay is the smallest value of T that satisfies the equations

$$T = \cos^{-1}(x)/w^{**} \quad \text{and} \quad T = \sin^{-1}(y)/w^{**} \quad (34)$$

Using Result 3.6, one can now obtain all the possible instances in which the system reaches the bound on the gain that is independent of time delay for the system with positive and negative feedback.

Though the above simple examples illustrate Results 3.4–3.6 for classically damped systems, the results presented in this section apply to non-classically damped systems as well. We showed that when the open loop system has all poles with negative real parts, and the controller transfer function is an analytic function, then there is a range in the gain for which the closed loop system is stable (even in the presence of time delays).

For the case of a single sensor with a single actuator, we showed that there is a range in the gain for which the system is stable for all time delays. This is provided the open loop system has all poles with negative real parts, and the controller transfer function satisfies some conditions.

The results imply that for the systems considered, all poles originate in the left complex plane and any pole in the right-half complex plane can be traced to the left-half complex plane by varying the gain.

The fact that for some systems the lower bound on the maximum gain for stability which is independent of time delay is achieved when no time delay is present (*Example 1*), suggests

that the use of a time delay may actually increase the maximum gain for stability when compared to the system with zero time delay for such systems. Therefore with an appropriate choice of time delay one could increase the range in the gain for which the system is stable, thereby making the use of time delays desirable. From a control design point of view, this could improve the control performance dramatically for such systems.

4. EXPERIMENTS WITH A NON-CLASSICALLY DAMPED, 2-DOF TORSIONAL SYSTEM

The effect of time delay on the control of a 2-degrees-of-freedom (2-DOF) torsional bar is explored experimentally and numerically. The maximum gain for stability is determined experimentally over a range of time delays for collocated integral and non-collocated derivative control and this is compared to analytical/numerical predictions based on a model of the system. For the case of collocated integral control, it is found both experimentally and numerically that a pole of the structural system, which *does not* originate from an open loop pole, dictates the maximum gain for stability for some time delays. In this section we first provide a description of the apparatus including a mathematical model. Following this, the experimental procedure is summarized. Finally, the experimental and numerical results are presented. Additional experimental and numerical results on collocated and non-collocated proportional, derivative and integral control of the torsional bar can be found in von Bremen *et al.* [16].

In the absence of any time delays, the system has two-degrees-of-freedom (with 2 sets of system poles). However, in the presence of time delays in the control loop, this seemingly simple system has a complex behavior for it is no longer finite dimensional. It has an infinite number of poles, and as the control gain increases from zero these poles ‘stream in’ from $-\infty$ in the left half complex plane towards the imaginary axis. As we will show, their root loci can ‘collide’ with those of the system poles, thereby leading to interesting behavior, and bifurcations.

4.1. Experimental setup and model

The setup (Figure 10) consists of 2 discs that undergo torsional vibrations. The inertial properties of the disks can be altered by fastening additional weights to them. The control system has four primary components: (1) the real-time controller that generates the input trajectory and computes the control algorithm, (2) the software for defining the controller, (3) the actuator at the lower disc, and (4) the optical sensors. The real-time controller is a digital signal processor-based single-board computer. The servo loop closure involves the computation of the user-supplied control algorithm, and these computations occur at a rate of once every sampling period (0.00442 s).

The actuator that actuates the lower disk utilizes a brushless dc motor with electrical commutation. Electrical commutation is accomplished by a sinusoidal switching scheme which has the advantage of reducing the magnitude of torque ripple. A sensor is secured to the motor shaft and reads its position. There are four incremental rotary shaft optical encoders on the system. Three are used to sense the position of the rotating disks. They have a

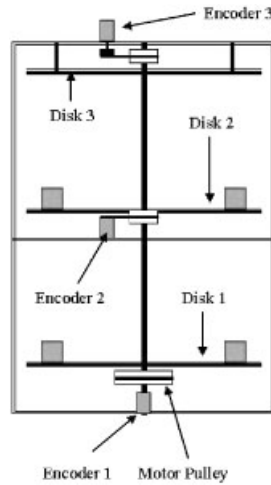


Figure 10. Experimental apparatus.

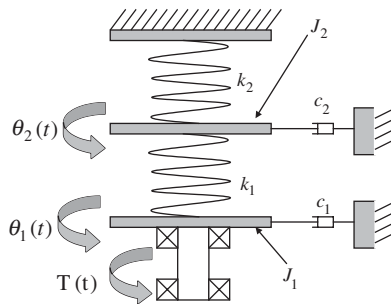


Figure 11. Model of experimental apparatus.

resolution of 4000 pulses per revolution. The fourth encoder, with a resolution of 1000 pulses per revolution, is connected to the motor.

Accompanying the experimental results is a numerical study of the system. A model of the experimental apparatus appears in Figure 11. The equations of motion of the two masses in Figure 10 are as follows:

$$\begin{aligned} J_1 \theta_1'' + c_1 \theta_1' + k_1(\theta_1 - \theta_2) &= T_c(t) \\ J_2 \theta_2'' + c_2 \theta_2' + k_1(\theta_2 - \theta_1) + k_2 \theta_2 &= 0 \end{aligned} \quad (35)$$

Here, J_i , $i = 1, 2$, are the mass moments of inertia of the disks; c_i , $i = 1, 2$, are the respective viscous damping coefficients; k_i , $i = 1, 2$, are the stiffness coefficients; θ_i , $i = 1, 2$, are the angular displacements of the disks; and $T_c(t)$ is the actuator torque.

Table I. Experimentally determined system parameters.

System parameter	Experimental value
J_1	0.00252 kg m ²
J_2	0.00194 kg m ²
k_1	2.830 N m/rad
k_2	2.697 N m/rad
c_1	0.00659 N m s/rad
c_2	0.00229 N m s/rad

The actuator control torque for non-collocated derivative and for collocated integral control is respectively of the form

$$T_c(t) = -\mu\theta_2'(t-T) \quad \text{and} \quad T_c(t) = -\mu \int_0^t \theta_1(\tau-T) d\tau \quad (36)$$

In both cases, μ is the control gain and T is the time delay in the control.

The system parameters are estimated by clamping each disk, in turn, and measuring the vibratory responses. These results are found in Table I. Though only a two degree-of-freedom system, it is non-classically damped.

4.2. Control procedure

Derivative control requires the estimation of the response derivative in real time. The following numerical approximation was used to compute the derivative $\theta_2'(t-T)$:

$$\theta_2'(t-T) = \frac{1}{2h} \{ \theta_2(t-(2h+T)) - 4\theta_2(t-(h+T)) + 3\theta_2(t-T) \} + O(h^2)$$

Here $h = T_s$ (with $T_s = 0.00442$ s) and T is the time delay. Using the above expression for the derivative, the control effort with control gain μ for non-collocated derivative control using a time delay of T becomes

$$T_c(t) = -\frac{\mu}{2T_s} \{ \theta_2(t) - (2T_s + T) - 4\theta_2(t - (T_s + T)) + 3\theta_2(t - T) \} \quad (37)$$

Integral control requires the estimation of the integral. The trapezoidal rule is used to approximate the integral as

$$\int_0^{nh} \theta_1(\tau-T) d\tau = \frac{h}{2} \left\{ \theta_1(-T) + \sum_{j=1}^{n-1} \theta_1(jh-T) + \theta_1(nh-T) \right\} + O(h^2)$$

Again, $h = T_s$ and T is the time delay. Recall that the system is initially at rest, so for $t < 0$, $\theta_1(t) \equiv 0$. Using the expression for the integral and the last observation, the control

effort for collocated integral control with a time delay of T is

$$T_c(t) = -\frac{\mu T_s}{2} \left\{ \sum_{j=1}^{n-1} \theta_1(jT_s - T) + \theta_1(nT_s - T) \right\} \quad (38)$$

In order to implement a time delay in the control, the control algorithm stores disk positions for previous sampling periods. Then, when defining the control law as in Equations (37) and (38), this past data is utilized. This means, however, that one is limited to time delays that are multiples of the sampling period.

The system described above is equipped with a safety feature which aborts control if the flexible shaft is over deflected or if the speed of the motor is too high. This was taken into account when the stability of the system was to be determined. A stable system was one where the amplitudes of motion would decrease with time. An unstable system was one where the amplitudes of motion increased with time, often leading to the safety limits being exceeded.

4.3. Experimental results

The maximum gain for stability of the system over a range of time delays is experimentally determined when using collocated integral control and non-collocated derivative control. These experimental results are compared to numerical predictions of the maximum gain for stability of the system and, in general, there is close agreement for a wide range of time delays.

We also present numerical results that help us understand the effect that time delays have on the stability of the system. The numerical results presented deal with bifurcations, and the fact that a *non-system pole* (a pole whose root locus does not originate at an open loop pole of the structural system) can dictate the maximum gain for stability for the closed loop system. A system pole is simply a pole whose root locus originates at an open loop pole of the structural system. Non-system poles include poles that originate at the poles of the controller, and those caused by the presence of the time delay.

When increasing the gain from zero, the pole that first crosses the imaginary axis will be called the dominant pole. This pole in essence limits the range of the gain for which the system is stable. Intuitively, one might expect that the dominant pole to be a system pole, because system poles are directly related to the physical structure and the non-system poles are induced by the controller and the time delay.

The open loop poles of the system when using the experimental parameter values from Table I are at $s_{1,2} = -0.7482 \pm 59.4029 i$, and at $s_{3,4} = -1.1495 \pm 21.0010 i$. Note that the poles come in conjugate pairs, and this will be the case for all the poles including the non-system poles. On root loci plots, the location of the open loop poles will be denoted with the symbol ‘*’ (making it easy to identify the root locus corresponding to a system pole). The system poles will usually be traced using a thick line, while the non-system poles with a thin line. In this subsection, all the time delays are given in units of seconds, and frequencies in rads/s.

Tracking the system poles as the gain changes is done simply by following the root loci of the poles starting at an open loop pole. However, the task of tracking non-system poles is a difficult one, since we may have infinitely many of them, and there is no systematic way

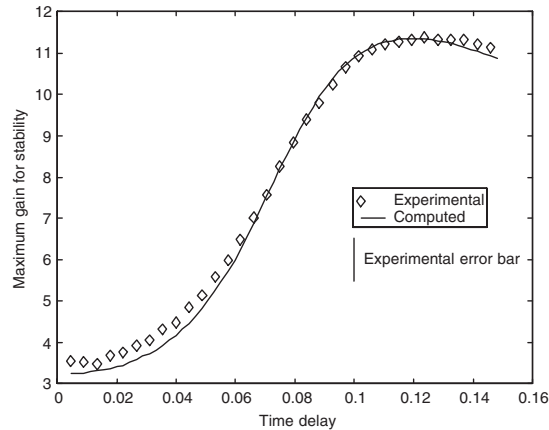


Figure 12. Experimental maximum gain for stability versus time delay for integral collocated control.

of selecting an initial location for all the poles[‡] and tracing them by varying the gain (as for system poles). The non-system poles that originate at the poles of the controller or end at the zeros of the controller can, however, be traced in the usual way.

Collocated integral control. Figure 12 represents a plot of the experimental results for time delay versus the maximum gain for stability under collocated integral control. The solid line on the plot is numerically determined using the system model described above. According to the numerical results, then, a coordinate pair (time delay, gain) which finds itself above the line is unstable, and one below the line is stable. The experimental maximum gain for stability is also depicted on this graph as data points.

The numerical results show a trend of increasing maximum gain for increasing time delay until about 0.12 s. where the gain begins to decrease. The curve of the maximum gain for stability suggests that one can properly choose a time delay that can give the system a *larger* maximum gain for stability than the one the system has for no time delay.

A root locus of a pole that starts (when the gain is close to zero) in the left-half complex plane may cross the imaginary axis several times (as the gain is increased). The value of the pole (on a root locus) in the complex plane when it crosses from the left-half (complex) plane to the right-half (complex) plane for the first time, as the gain is increased gradually from zero, will be called the cross-over frequency. Figures 13 and 14 show the maximum gain for stability and the cross-over frequency versus time delay for collocated integral control, when only system poles are considered. The points denoted by 'o' correspond to system poles originating at s_1 , and the points denoted by '*' correspond to the system pole originating at s_3 (due to symmetry, the conjugates of these two system poles are also present in the system). Similar plots are given in Figures 15 and 16, which show the maximum gain for stability and the cross-over frequencies versus time delay for collocated integral control, when all (system and non-system) poles are considered. Even though the system does not satisfy all the required conditions of Result 3.4, the maximum gain for stability which is independent of time delay,

[‡]By means of Jensen's formula (see Rudin [17, p.307]) it is possible to determine the magnitude of the non-system poles at given gains and time delays for special systems.

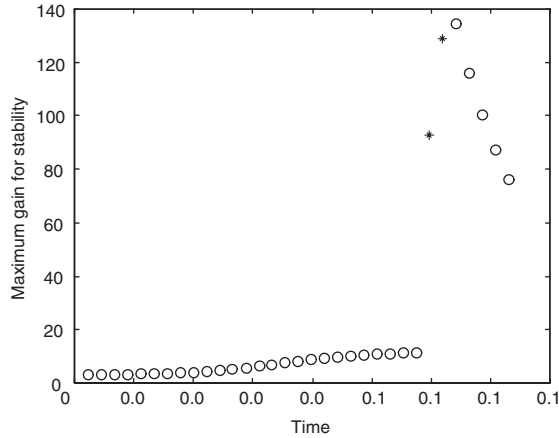


Figure 13. Maximum gain for stability versus time delay for collocated integral control using system poles only.

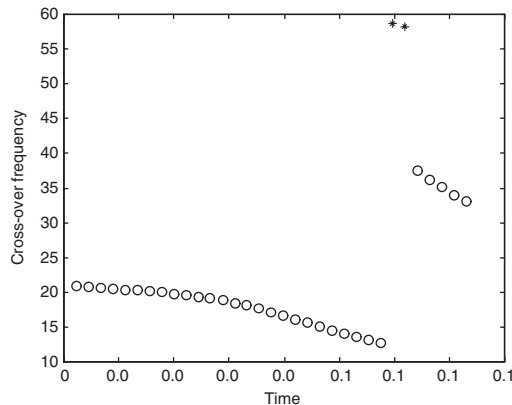


Figure 14. Cross-over frequency versus time delay for collocated integral control system poles only data.

given by Result 3.4 is found to be 3.266. This is also exactly the numerically expected value (Figure 15) and it is very close to the experimentally observed value. We note that at zero time delay, the smallest maximum gain for stability is achieved (see Figures 12, 13 and 15).

Figures 15 and 16 are smooth continuous curves, while Figure 13 and 14 seem discontinuous and present abrupt changes. The difference between the system-poles data and the all-poles data plots suggest that there is a range in the time delay where a non-system pole is the dominant pole. This expectation is confirmed by plots in Figures 17 and 18, which show the root locus of the system poles (thick lines) and two non-system poles (thin lines) for time delays of 0.11 and 0.13 s, respectively. The root loci are taken for values of the gain μ between 0 and 50, except for the portion of the root loci that lies on the horizontal axis,

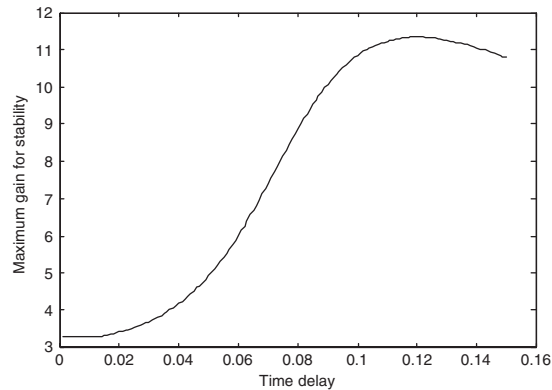


Figure 15. Maximum gain for stability versus time delay for collocated integral control, including all poles.

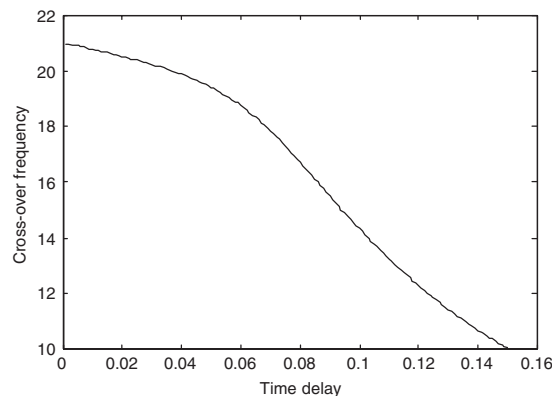


Figure 16. Cross-over frequency versus time delay for collocated integral control, including all poles.

where the initial gain is larger than 0 in order to avoid problems of scaling. For the time delay of 0.11 s, two system poles cross the imaginary axis first, that is, the dominant poles are two conjugate system poles (see Figure 17), while for a time delay of 0.13 s, two conjugate non-system poles have become dominant (see Figure 18).

The fact that there is an exchange of dominant pole status between a system pole and a non-system pole, suggests the existence of a bifurcation. This bifurcation is presented in Figure 19 which shows the root loci for a system pole (thick line) and a non-system pole (thin line) at different time delays. The system pole root locus starts at a gain of zero, while the portion of the non-system pole displayed starts from the horizontal axis with a gain larger than zero. The maximum gain is 50 for both poles. A bifurcation occurs at a time delay of about 0.11265 s. The poles selected are such that the system pole is the dominant pole for time delays less than 0.112 s and the non-system pole is the dominant pole for time delay

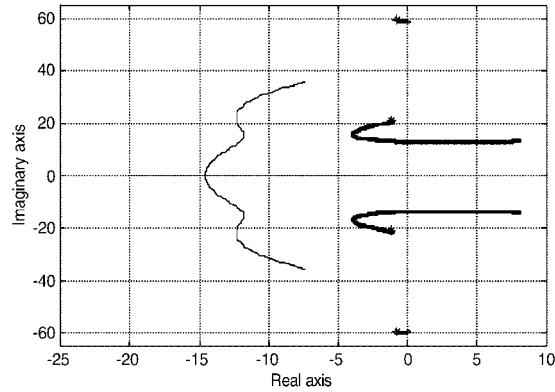


Figure 17. Root locus of the system poles and two non-system poles for time a delay of 0.11 s, using collocated integral control.

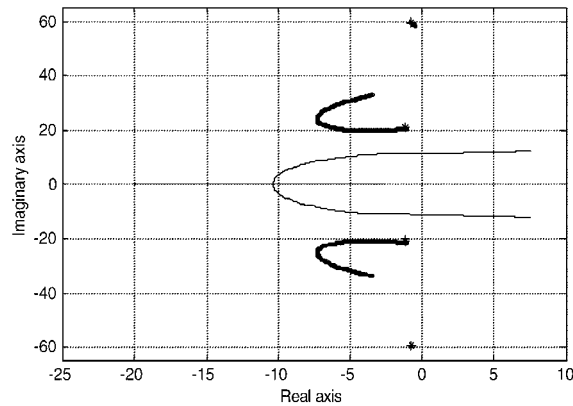


Figure 18. Root locus of the system poles and two non-system poles for time a delay of 0.13 s, using collocated integral control.

greater than 0.113 s. Initially (for small time delays), the system pole is the dominant pole, as the time delay is increased the root loci of the two poles move closer until they touch (approximately at a time delay of 0.11265 s). This is the point where the bifurcation occurs. At the bifurcation, one ‘arm’ of the root loci is exchanged among the two poles. The system pole gives the ‘arm’ that dictates the maximum gain for stability to the non-system pole, and the non-system poles gives the slow moving ‘arm’ to the system pole. After the exchange of ‘arms’ at the bifurcation, the root loci of the two poles move apart as the time delay is increased.

To confirm that a non-system pole is actually the dominant pole, two experiments are conducted on the two-degree-of-freedom torsional bar. The system is fed a sine wave with a given frequency, and the steady state amplitude of the response of disk 1 is recorded for

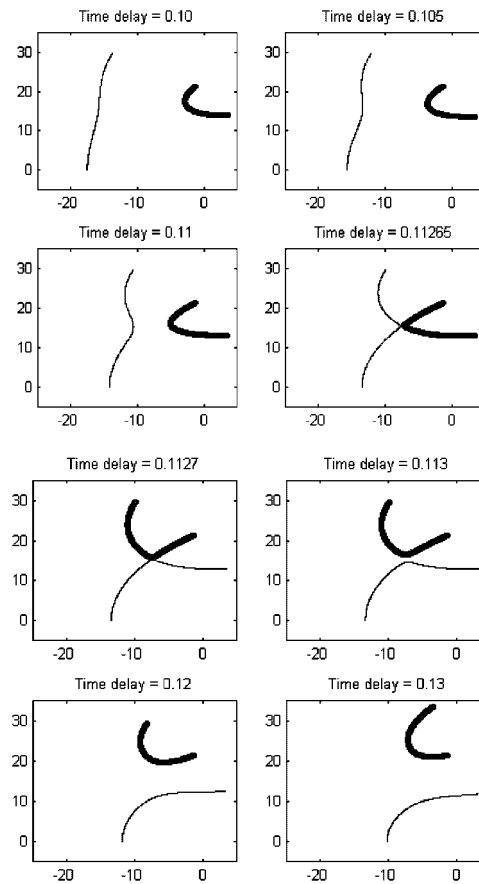


Figure 19. Root loci for different time delays showing bifurcation for collocated integral control.

different gains, while the control effort is active. The experiments are conducted using three different frequencies. These chosen frequencies are the cross-over frequencies for two of the system poles (originating from s_1 and s_2) and a non-system pole at a given time delay. Recall that the cross-over frequency is defined as the purely imaginary value of a pole (moving along a root locus, and starting in the left-half complex plane) when it first crosses the imaginary axis, as the gain is gradually increased from zero. The time delays are taken to be 0.11 s in the first experiment and 0.13 s in the second. The objective is to experimentally confirm the location of points on the root locus.

The results for a time delay of 0.11 s are shown in Figure 20. The frequencies of 13.2 and 59.7 rad/s correspond to the cross-over frequencies of the system poles, while the frequency of 43.6 rad/s is the cross-over frequency for the non-system pole. As expected, when the system is excited near the frequency of the dominant pole, and at a gain close to the maximum gain for stability, the amplitude of the response increases drastically. However, when the system is excited at a frequency which is 'far' from the cross-over frequency, the amplitude of the

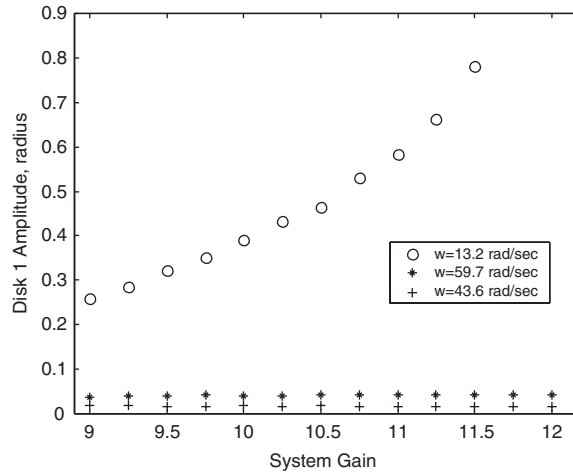


Figure 20. Amplitude of the steady state response of disk 1 versus gain for different frequencies of the sine wave using collocated integral control and a time delay of 0.11 s.

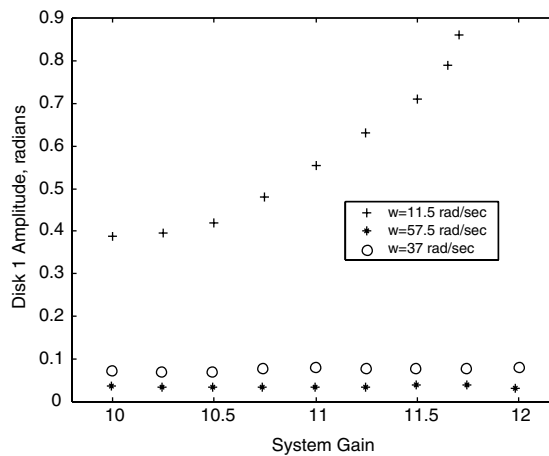


Figure 21. Amplitude of the steady state response of disk 1 versus gain for different frequencies of the sine wave using collocated integral control and a time delay of 0.13 s.

response does not increase greatly, even in the vicinity of the maximum gain for stability (as seen for the frequencies of 59.7 and 43.6 rad/s). This experiment confirms that for a time delay of 0.11 s, the dominant pole is a system pole which crossed-over at a frequency of about 13.2 rad/s.

The results for a time delay of 0.13 s are shown in Figure 21. The frequencies of 57.5 and 37 rad/s are the cross-over frequencies for the system poles and the frequency of 11.5 rad/s is the cross-over frequency of a non-system pole. The plot shows that the amplitude of the oscillations of disk 1 increases when the system is excited at the expected cross-over frequency

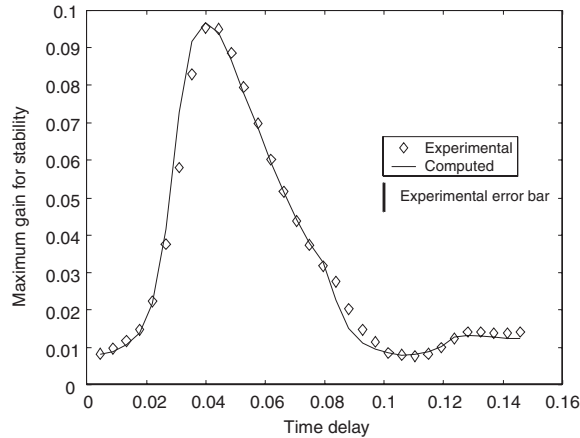


Figure 22. Experimental maximum gain for stability versus time delay for non-collocated derivative control.

of the non-system pole near the maximum gain for stability. On the other hand, when the system is excited at the cross-over frequencies of the system poles (which are not dominant), the amplitude of the response remains small and almost unchanged near the maximum gain for stability corresponding to the dominant pole. This behavior confirms the expectation that at a time delay of 0.13 s, a non-system pole is the dominant pole.

The experimental results show that a non-system pole can be the dominant pole for collocated integral control, and that our analysis can predict this behavior. Also, the maximum gain for stability *with* time delays is much higher than in the absence of a time delay. The behavior of the system can be theoretically explained in terms of bifurcation diagrams.

Non-collocated derivative control. Figure 22 represents a plot of time delay versus the maximum gain for stability for non-collocated derivative control. As before, the solid line depicts a numerically generated estimate of the maximum gain for stability as a function of time delay. The data points represent experimentally determined values for the maximum gains for stability at various time delays.

The numerical results show a trend of increasing maximum gain for increasing time delay until about 0.04 s where the gain decreases. Thus a proper choice of time delay can give the system a much *larger* maximum gain for stability than if there were no time delay.

Figure 23 shows the numerically determined maximum gain for stability versus time delay for the torsional bar using non-collocated derivative control. For the time delays shown, the dominant pole is always a system pole. Again, points denoted by 'o' correspond to system poles originating at s_1 , and the points denoted by '*' correspond to the system pole originating at s_3 . In the range of time delays shown, there are three instances in which the dominant pole changes from one system pole to another. The changes occur at time delays of about 0.04, 0.08 and 0.125 s. Figure 24 shows the expected cross-over frequency (frequency of the dominant pole at the maximum gain for stability) versus time delay. The fact that the dominant pole changes from one system pole to another suggests the presence of bifurcations at the locations where the changes occurs.

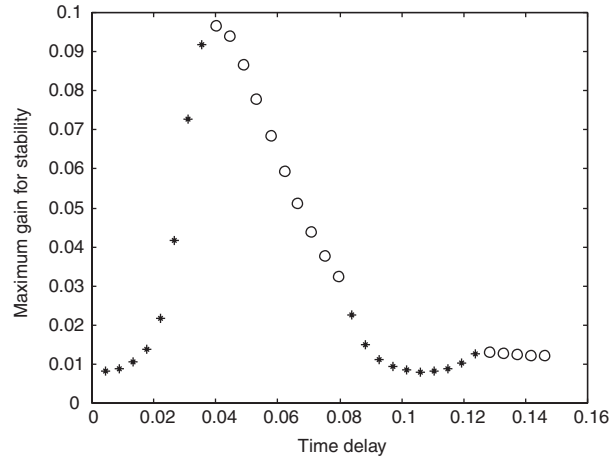


Figure 23. Expected maximum gain for stability versus time delay for non-collocated derivative control.

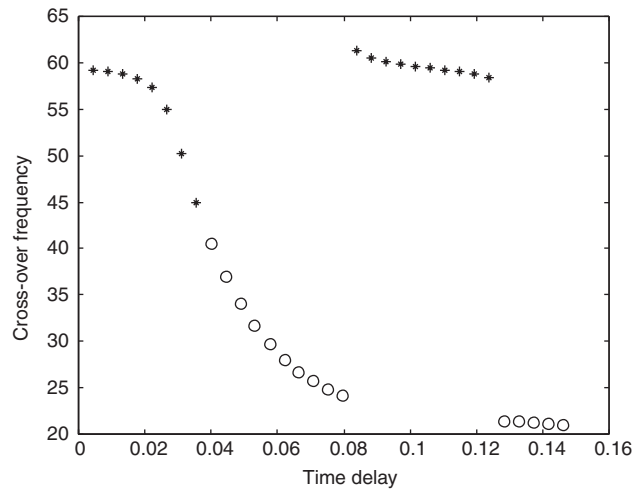


Figure 24. Expected cross-over frequency versus time delay for non-collocated derivative control, showing possible bifurcations at about 0.0396, 0.08 and 0.125 s.

The maximum gain for stability for non-collocated derivative control which is independent of time delay, given by Result 3.4 is 0.007988. When the time delay is zero, the above time-delay-independent maximum gain for stability is achieved (see Figures 22 and 23). There is close agreement between the computational results from this section and the results from the method of Section 3, with regards to the maximum gain for stability independent of time delay.

A bifurcation occurs at a time delay of about 0.0396 s. This bifurcation is shown on Figure 25, which shows the root loci of two of the system poles for different time delays.

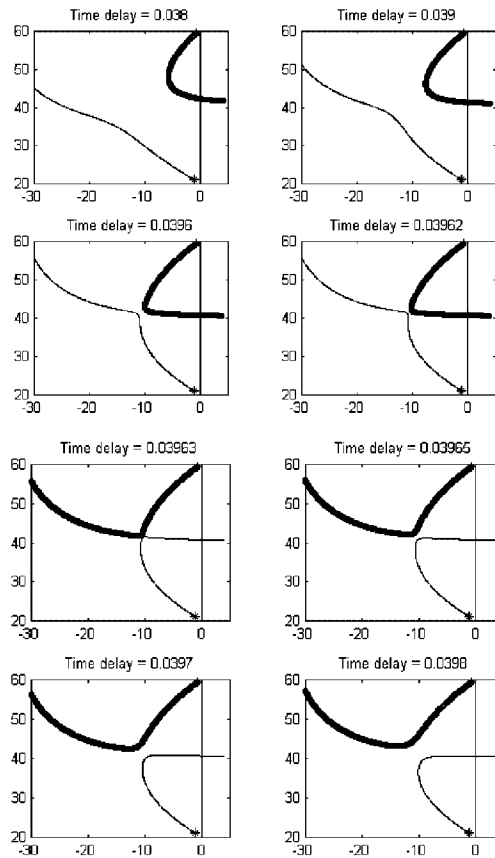


Figure 25. Root loci for different time delays showing bifurcation for non-collocated derivative control.

At the bifurcation, one ‘arm’ of the root loci is exchanged among the two system poles. The thick line represents the root locus for the pole originating at the open loop pole s_1 , while the thin line is the root locus for the pole originating at s_3 . The root loci correspond to gains between 0 and 0.12. The general behavior of the root loci of the poles at the bifurcation is similar to the one for collocated integral control (see Figure 19). The main difference between the two cases is that for collocated integral control, a system pole and a non-system pole are involved, while for the present case, only system poles are involved. At a time delay of about 0.08 s we have another bifurcation. However this bifurcation is less dramatic; there is no intersection of the root loci of the poles. The change of dominant pole occurs simply because there is a change in the rate at which the poles move across the complex plane.

The experimental and numerical results presented in this section show that for collocated integral control, there are time delays for which the dominant pole is a non-system pole. On the other hand, in the experiments with non-collocated derivative control, the dominant pole is a system pole (for the range in time delay considered). Good agreement between the experimental and the numerically expected maximum gain for stability is observed. For both,

collocated integral control and non-collocated derivative control (see Figures 12 and 22), the introduction of a suitable time delay, will yield a higher maximum gain for stability than the one for the system with no time delay. The next section deals with the control of time invariant systems with system uncertainties that include uncertainties in the time delay that is used. We model this uncertainty as a time-varying time delay.

5. CONTROL OF UNCERTAIN SYSTEMS

The models presented in Sections 2 and 3 do not include system uncertainties in the formulation. However, the numerical results presented in Section 2.5, suggest that structural systems may remain stable after the parameters of the system are slightly perturbed (or uncertain). This section deals with the robust state feedback control of time invariant dynamic systems with time varying control delays and system uncertainties. Corless and Leitmann [18], Gutman and Leitmann [19], and Chen and Chen [20] have worked on control systems which deal with uncertainties embedded in the system's structure or with externally introduced uncertainties (like measurement noise). In this section we introduce a new set of uncertainties in the system, in terms of the time delay in the control. Here the time delay in the control is allowed to be a bounded function of time.

Consider the system whose response $x(t)$ is governed by the matrix differential equation

$$x'(t) = Ax(t) + \Delta Ax(t) + Bu(t) + \Delta Bu(t) + \delta Bu(t - h(t)) \quad (39)$$

where the m -vector $u(t)$ is the control function, the matrices ΔA , ΔB , δB have uncertain entries and $h(t)$ is the time-varying time delay. The matrices A , and ΔA are n by n , B , ΔB and δB are n by m , and $x(t)$ is an n -vector.

The elements of the uncertain matrices could either have deterministic or stochastic forms. Thus the stochastic uncertainties which are usually present in the stiffness and damping matrices can be included in the matrices ΔA .

Assume that

$$\begin{aligned} \Delta A &= BD \quad \text{with } \|D\| = k_1, \quad k_1 \in [0, \infty) \\ \Delta B &= BE \quad \text{with } \|E\| = k_2, \quad k_2 \in [0, 1) \\ \delta B &= BF \quad \text{with } \|F\| = \tilde{k}_2, \quad \tilde{k}_2 \in [0, \infty) \end{aligned} \quad (40)$$

The above assumptions on the norms of the matrices can be interpreted as, the uncertainties in the system are bounded by known constants k_1, k_2 and \tilde{k}_2 . The restriction that $k_2 \in [0, 1)$ is interpreted as follows: the uncertainty in the control cannot be so severe as to reverse the direction of the control action, for then one is not able to tell if the control is in the desired direction.

If the state feedback control $u(t)$ is chosen as

$$u(t) = -\frac{1}{2} \sigma B^T P x(t) \quad (41)$$

where P is the solution of the Lyapunov equation,

$$A^T P + PA = -(Q + H), \quad P, Q, H > 0 \quad (42)$$

then the response of system (39) is stable, provided that the following conditions are satisfied.

$$h(t) < h_0, \quad h'(t) \leq a < 1 \quad \text{and} \quad \rho > 4\eta^2 \quad (43a)$$

where

$$\eta^2 = \frac{\tilde{k}_2^2 \|B^T P\|^2}{4(1-a)\lambda_{\min}(H)} \quad \text{and} \quad \rho = \frac{(1-k_2)^2 \lambda_{\min}(Q)}{k_1^2}$$

The control gain is chosen as

$$\sigma \leq \frac{(1-k_2)}{\eta^2 + \theta}, \quad \theta > 0 \quad (43b)$$

where θ is a positive constant which has to satisfy the condition,

$$\frac{\rho - 2\eta^2}{2} \{1 - \sqrt{1 - \Omega^2}\} < \theta < \frac{\rho - 2\eta^2}{2} \{1 + \sqrt{1 - \Omega^2}\}$$

here

$$\Omega = \frac{2\eta^2}{\rho - 2\eta^2}$$

The result presented shows that systems with uncertainties in the parameters and in the time-delayed controller can be stabilized under special conditions. For a proof of the result and numerical simulations which validate it, see Udwadia *et al.* [21] and Udwadia and Hosseini [22].

6. CONCLUSIONS

In this paper we have studied time-delayed control of structural systems from several viewpoints. We show that the *purposeful injection* of time delays can indeed improve both the stability and performance characteristics of controlled systems. Rather than developing complex schemes to eliminate, compensate for, or nullify time delays (as has been the traditional view), we show analytically, numerically, and experimentally that time delays can be purposefully and intentionally used to good advantage. This becomes more so important because time delays are indeed ubiquitous in control systems. Furthermore, we show that such time delayed control can be made robust with respect to uncertainties in the system's parameters and uncertainties in the implementation of the time delays themselves. We present next a detailed set of conclusions.

Section 2 deals with the control of classically damped structural systems. Results for collocated and non-collocated control of damped and undamped multi-degree-of-freedom systems were given. For undamped and underdamped system, several analytical conditions on the time delay that guarantees that the closed loop system poles move to the left in the complex plane are given. Since PID control is one of the most commonly used control laws in practice, we use this controller to obtain conditions when time delays can stabilize undamped systems. We illustrate our results using numerical computations. We show that non-collocated derivative control that is unstable in the absence of time delays can be made stable through the

simple introduction of suitable, intentional time delays. The robustness of time delayed control to variations in the values of the structural parameters (mass and stiffness) and the time delay itself is numerically explored for non-collocated derivative control. The results show that even under considerable perturbations of the parameter values the system remains stable.

General non-classically damped systems are treated in Section 3. The results presented deal with the case of one actuator, and the transfer function of the controller is assumed to be an analytic function. The main results can be summarized as follows: (1) When all the poles of the open loop system have negative real parts and the controller transfer function is an analytic function, then for any given time delay there exists a range in the gain (which is, in general, dependent on the given time delay) for which the closed loop system is stable. (2) For a single actuator and a sensor under the same conditions as before, there is an interval of gain which is independent of time delay for which the system is stable. This gain can be computed without knowledge of the time delay. (3) We show that through a proper choice of time delay, one may obtain a larger maximum gain for stability than the one for the system with no time delay. Thus the injection of a time delay could significantly improve the performance of the control of such a system.

Experimental and numerical results on the control of a two-degree-of-freedom torsional bar are presented in Section 4. The main results are summarized as follows: (1) Experimental results showing the maximum gain for stability versus time delay, for both collocated integral control and non-collocated derivative control, exhibit close agreement with the numerical/analytical expectations. Furthermore, the results show that the presence of a time delay will actually increase the maximum gain for stability, when compared with the maximum gain for stability when the system has no time delay. (2) For non-collocated derivative control, we numerically find that the dominant pole (the pole that dictates the maximum gain for stability) is always a system pole (for the range of time delays analysed). For different time delays the dominant pole may change from one system pole to another. At these time delays we have bifurcations. (3) For collocated integral control, we numerically find that the dominant pole can be a non-system pole. This result is corroborated by actual experiments. As with the non-collocated case, the dominant pole changes as the time delay is varied, and now bifurcations involving system and non-system poles occur. We illustrate such a bifurcation both experimentally and computationally.

Finally, Section 5 deals with the robust state feedback control of time invariant structural systems with time-varying time delays and system uncertainties. A state feedback control is suggested that guarantees the stability of the system, provided, principally, the so-called matching conditions are met.

Even though we have taken different approaches when dealing with the time-delayed control of structural systems, throughout this paper there is the recurring theme that under an appropriate choice of time delay, the maximum gain for stability could be greater than the maximum gain for stability obtained when no time delay is used. Since time delays are ubiquitous in the control of large scale structural systems, this strongly suggests the idea that instead of trying to eliminate/nullify time delays, we may actually want to introduce them appropriately in order to provide stable non-collocated control. We also show that this increase in the maximum gain for stability in the presence of delays can improve the control performance especially for non-collocated control.

Our results, both experimental and analytical, indicate that the research presented in this paper will be of practical value in improving the performance and stability of controllers.

Through the proper purposive injection of small time delays, it is possible to dramatically improve the performance and stability of certain control systems. Furthermore, the injection of small time delays can be easily implemented in a reliable and nearly costless way on an already installed controller. Thus the performance and stability of active control systems that are already installed in building structures can be enhanced in a nearly costless way by including appropriate and intentional time delays in the feedback loop. This makes the method very attractive from an economic and safety retro-fit standpoint when dealing with the active control of structural systems subjected to strong earthquake ground shaking.

REFERENCES

1. Auburn JN. Theory of the control of structures by low-authority controllers. *Journal of Guidance and Control* 1980; **3**:444–451.
2. Balas MJ. Direct velocity feedback control of large space structures. *Journal of Guidance and Control* 1979; **2**:252–253.
3. Balas MJ. Direct output feedback control of large space structures. *The Journal of Astronomical Sciences* 1979; **XXVII**(2):157–180.
4. Goh CJ, Caughey TK. On the stability problem caused by finite actuator dynamics in the collocated control of large space structures. *International Journal of Control* 1985; **41**(3):787–802.
5. Fanson JL, Caughey TK. Positive position feedback control for large space structures. *AIAA Journal* 1990; **28**(4):717–724.
6. Cannon RH, Rosenthal DE. Experiments in control of flexible structures with noncolocated sensors and actuators. *Journal of Guidance and Control* 1984; **7**:546–553.
7. Yang JN, Akbarpour A, Askar G. Effect of time delay on control of seismic-excited buildings. *Journal of Structural Engineering (ASCE)* 1990; **116**(10):2801–2814.
8. Agrawal AK, Yang YN. Effect of fixed time delay on stability and performance of actively controlled civil structures. *Earthquake Engineering and Structural Dynamics* 1997; **26**:1169–1185.
9. Agrawal AK, Fujino Y, Bhartia BK. Instability due to time delay and its compensation in active control of structures. *Earthquake Engineering and Structural Dynamics* 1993; **22**:211–224.
10. Agrawal AK, Yang YN. Compensation of time-delay for control of civil engineering structures. *Earthquake Engineering and Structural Dynamics* 2000; **29**:37–62.
11. Kwon WH, Lee GW, Kim SW. Delayed state feedback controller for the stabilization of ordinary systems. *Proceedings of the American Control Conference*, vol. 1, Pittsburgh, Pennsylvania, 1989; 292–297.
12. Udwadia FE, Kumar R. Time delayed control of classically damped structural systems. *International Journal of Control* 1994; **60**(5):687–713.
13. Udwadia FE, Kumar R. Time delayed control of classically damped structures. *Proceedings of the 11th World Conference of Earthquake Engineering*, Acapulco, Mexico, 23–28 June, 1996.
14. von Bremen HF, Udwadia FE. Can time delays be useful in the control of structural systems? *Proceedings of the 41st AIAA/ASME/ASCE/AHS/ASC Structures, Structural Dynamics, and Materials Conference*, Atlanta, GA, 3–6 April, 2000.
15. Ahlfors LV. *Complex Analysis*. McGraw-Hill: New York, 1979.
16. von Bremen HF, Udwadia FE, Silverman MC. Effect of time delay on the control of a torsional bar. *Proceedings of the 42nd AIAA/ASME/ASCE/AHS/ASC Structures, Structural Dynamics, and Materials Conference*, Seattle, Washington, 16–19 April, 2001.
17. Rudin W. *Real and Complex Analysis*. McGraw-Hill: New York, 1987.
18. Corless MJ, Leitmann G. Continuous state feedback guaranteeing uniform ultimate boundedness for uncertain dynamic systems. *IEEE Transactions on Automatic Control* 1981; **AC-26**(5):1139–1144.
19. Gutman S, Leitmann, G. Stabilizing control for linear systems with bounded parameter and input uncertainty. *Proceedings of the 7th IFIP Conference on Optimization Techniques*. Springer Verlag: Berlin, 1976.
20. Chen YH, Chen JS. Adaptive robust control of uncertain systems. *Control and Dynamic Systems* 1992; **50**: 175–222.
21. Udwadia FE, Hosseini MAM, Chen YH. Robust control of uncertain systems with time varying delays in control input. *Proceedings of the 1997 American Control Conference*, Albuquerque, New Mexico, 4–6 June, 1997.
22. Udwadia FE, Hosseini MAM. Robust stabilization of systems with time delays. *ASCE Proceedings of the seventh specialty conference, Probabilistic Mechanics and Structural Reliability*, Worcester, MA, 7–9 August, 1996; 438–441.